UPPSALA
UNIVERSITET

A hydropower perspective on flexibility demand and grid frequency control

Linn Saarinen

UPPSALA
UNIVERSITET

A hydropower perspective on flexibility demand and grid frequency control

Linn Saarinen

UURIE 339-14L
ISSN 0349-8352
Division of Electricity
Department of Engineering Sciences
Uppsala, December 2014

Abstract

The production and consumption of electricity on the power grid has to balance at all times. Slow balancing, over days and weeks, is governed by the electricity market and carried out through production planning. Fast balancing, within the operational hour, is carried out by hydropower plants operating in frequency control mode. The need of balancing power is expected to increase as more varying renewable energy production is connected to the grid, and the deregulated electricity market presents a challenge to the frequency control of the grid.

The first part of this thesis suggests a method to quantify the need for balancing or energy storage induced by varying renewable energy sources. It is found that for high shares of wind and solar power in the system, the energy storage need over a two-week horizon is almost 20% of the production.

The second and third part of the thesis focus on frequency control. In the second part, measurements from three Swedish hydropower plants are compared with the behaviour expected from commonly used power system analysis hydropower models. It is found that backlash in the guide vane and runner regulating mechanisms has a large impact on the frequency control performance of the plants.

In the third part of the thesis, the parameters of the primary frequency control in the Nordic grid are optimised with respect to performance, robustness and actuator work. It is found that retuning of the controller parameters can improve the performance and robustness, with a reasonable increase of the actuator work. A floating deadband in the controller is also discussed as a means to improve performance without increasing the actuator work.

List of papers

This thesis is based on the following papers, which are referred to in the text by their Roman numerals.

I L. Saarinen, N. Dahlbäck and U. Lundin. "Power system flexibility need induced by wind and solar power intermittency on time scales of 1-14 days." *Submitted to Renewable Energy*, July 2014.

II L. Saarinen, P. Norrlund and U. Lundin. "Field measurements and system identification of three frequency controlling hydropower plants." *Submitted to IEEE Transactions on Energy Conversion*, September 2014.

III L. Saarinen and U. Lundin. "Robust primary frequency control in a system dominated by hydropower." *Submitted to Control Engineering Practice*, November 2014.

Contents

Abbreviations

Symbol	Unit	Description
D		Load damping constant, load frequency dependency
E_p	Hz/MW	Droop, inverse static gain of controller
Ep0, Ep-läge		Frequency controller parameter settings
f	Hz	Grid frequency
FCR-D		Frequency containment reserve, disturbed operation
FCR-N		Frequency containment reserve, normal operation
FRR-a		Frequency restoration reserve, automatic
FRR-m		Frequency restoration reserve, manual
K_i	s	Integral gain of controller
K_p	pu	Proportional gain of controller
LFC		Load frequency control, secondary control
M	s	System inertia
n		Measurement disturbance
P	MW	Power
PID		Proportional, integral, derivative controller
PV		Photovoltaics
r	pu	Reference signal (grid frequency)
S_k		Energy storage need over the time horizon k
T_f	s	Input filter time constant
T_i	s	Feedback time constant of controller
T_p	s	Time constant of P-model
T_w	s	Water time constant
T_y	s	Servo time constant
TSO		Transmission system operator
u	pu	Control signal, guide vane opening
u_{pos}	pu	Guide vane position (after backlash)
u_p	pu	Grid input signal, power output from plant
VRE		Varying renewable energy
w		Output disturbance, grid frequency disturbance
w_u		Input disturbance, load disturbance
WP		Wind power
y	pu	Output signal, grid frequency
Y	%	Guide vane opening
Y_c	%	Guide vane opening control signal
Y_{mv}	%	Guide vane opening measured value
Y_{pos}	%	Guide vane opening position

1. Introduction

At all times, the production and consumption of electricity on the power grid have to be in balance. A small amount of energy is stored as kinetic energy in the rotation of the large machines that are directly connected (without inverter) to the grid, and any mismatch of production and consumption will lead to acceleration or deceleration of the whole system and thereby adding to or borrowing from the rotational energy of the system. The rotational speed of the machines, and thereby the electrical frequency of the grid, has to be kept close to its nominal value (50 Hz in the Nordic grid). Grid frequency deviations are especially harmful to thermal power plants, and if the grid frequency drops too low, they will disconnect in order to protect the machinery. If this happens, the grid frequency will start to drop even faster due to the increased mismatch between production and consumption, and eventually there will be a blackout. The objective of grid frequency control is to make sure that this never happens.

In the Nordic power system, grid frequency control is carried out mostly by hydropower plants. Hydropower can be regulated faster and with smaller loss of efficiency than most other power sources, and since there is plenty of hydropower in the Nordic system (especially in Norway and Sweden), it takes on most of the regulation task. However, there is an increasing concern among hydropower owners that the frequency control wears the turbines down. There have been several premature failures of Kaplan turbine runners in recent years, and increased grid frequency control activity is believed to be one of the reasons.

From the power system point of view, there are also challenges for the grid frequency control. The quality of the Nordic grid frequency, measured in minutes outside the normal operation band 49.9-50.1 Hz, has been gradually deteriorated during the last decades. There are several possible explanations for this, for example: The deregulation of the electricity market has led to more activity on the production side (starts and stops and load changes), especially around the hour shifts, since electricity is bought and sold in blocks of one hour; the production with varying renewable energy sources such as wind power, which need to be balanced, has increased; the amplitude of very low frequency oscillations of the grid frequency (period of 40-90 s) has increased; the operation of the grid frequency control might have changed due to the deregulation of the market, as the production companies gradually adjust to the new market situation.

The aim of this thesis is to start in the system we have today, with a diverse fleet of hydropower plants regulating the grid frequency with relatively simple

PI controllers, and find improvements that are easily implemented and beneficial for both the plants and the grid. One of the basic principles in process control is to "try simple things first", because the greater part of the possible improvement of the control of a process can often be achieved by good tuning of simple controllers. This thesis aims at this low hanging fruit, and the results are meant to form a baseline to which more advanced control strategies can be compared. This strategy also applies to the modelling approach of the thesis. The principle is to use models that are good enough for the application - not too simplified and not unnecessarily complex. One part of the thesis is focused on comparing the models to measurements on real plants, in order to find out what needs to be included in the model to actually describe the reality well enough.

The aim of the thesis is also to make an outlook on the future needs for balancing and frequency control. The challenge is primarily to balance the production from an increasing amount of varying renewable energy sources in the system. Since previous research has focused on the need for balancing over the intra-day or seasonal time horizon, the research on future needs in this thesis focuses on the 1-2 week time horizon.

A short note on the word frequency: In this thesis, two different frequency concepts are used: First; the grid frequency is the frequency of the voltages and currents of the grid, which are tightly connected to the speed of the machines. The Nordic grid frequency has a nominal value of 50 Hz, and it is the quantity one attempts to control with (grid) frequency control. Secondly, there is the frequency content of any signal (for exampel the frequency content of the grid frequency signal), derived from the Fourier transform of the signal. This is a means to describe the dynamic characteristics of the signal, that is, if it changes slowly or quickly in time. In this thesis, the word "frequency" will generally be used for the concept related to the Fourier transform, and "grid frequency" will be used for the concept of grid frequency. The exception to this principle is the widely established notion "frequency control", which will be used instead of the somewhat cumbersome "grid frequency control".

1.1 Previous research

In recent years, there has been an upswing in research on power system balancing and control. One reason for this is the increase of varying renewable energy (VRE) production, and the outlook on a future system dominated by renewables.

The flexibility need of the power system can be divided into four categories which are related to different time scales: Planning, correction and backup, rampage and power system stability [1]. Increased VRE production has a potential impact on all four time scales.

The planning time horizon stretches from one or several years (use of hydropower reservoirs, fuel purchase for thermal and nuclear power) to day-ahead unit commitment and dispatch. In the Nordic power system, the electricity is sold on long-term fixed price contracts and on the NordPool spot market. Both the load and the power generated by naturally varying sources like wind, solar, wave and tidal power vary with the time of the day and the weather. Some part of the variations are predictable, and some are stochastic. Day-ahead weather forecasts can be reasonably reliable, but the exact timing of events, like the passing of a weather front, are often uncertain. For longer time horizons like 5 or 10 days, weather prognoses are often very uncertain.

With more varying power producers in the system, the role of dispatchable power plants is transformed from base load production to backup or balancing power. This means more part load operation and more starts and stops. For thermal power this is associated with lower efficiency, higher emissions, shorter lifetime due to thermal stress and lower incomes due to fewer equivalent full load hours per year. Ummels et al. [2] has analysed the dispatch pattern for thermal power in a system with high integration of wind power, showing an increased need for thermal plants to operate on minimal load, especially during the nights. For hydropower, increased regulation (primary control) and frequent starts and stops means lower efficiency and shorter lifetime due to wear. There is also a cost for low utilisation of the installed power.

Heide et al. [3,4] and Rasmussen et al. [5] has analysed the yearly storage and balancing need in an European power system with 100% VRE, the optimal mix of wind and solar power and the relation between storage need and VRE overcapacity. In another Danish study, the occurrence and length of periods with very high and very low net loads that can be expected in the Danish power system in 2025 was analysed [6]. The result showed that periods of negative net load for 2-7 days would be common, while longer periods of high load would occur less often.

Seasonal variations for wind power has also been studied, for example by Tande et al. [7], showing that for Norway, wind power production co-varies with the load (higher in the winter and lower in the summer), but that over several years, there is a correlation between dry years (low inflow to the hydropower reservoirs) and a years with less wind.

The correction and backup time horizon stretches from day-ahead to hour-ahead in the Nordic power system. Corrections to the spot market result, for example due to errors in the prediction of production or load, can be bought and sold on the NordPool balancing market, ELBAS. The need of balancing power due to varying wind power production over the correction and backup time horizon has been thoroughly researched. In general, the net load (load minus wind power) prediction error is analysed instead of the prediction error for wind power only. One method of analysis is to decompose the net load prediction error into periodic components of different frequency, by using the Fourier transform. This information can be used for sizing of energy storage

[8]. Several other methods for storage sizing and storage operations can be found in the literature [9–12]. Different sizes of storages have been suggested, ranging from 2 hours of wind power peak production and a power capacity of 22% for a Portuguese pumped hydro storage [10] to 30-90 minutes and 10% power capacity for the Hungarian power system [13] and 1-3 hours and 25% power capacity for a Danish wind farm, using a dynamic sizing method [14]. For the Nordic countries, the increased reserve requirement at 10% wind energy penetration level has been estimated to 1.5-4% of installed wind power capacity [15].

Rampage can be seen as a special requirement within the correction and backup time horizon. When a weather front passes over a wind farm, the production will change with a certain ramp speed and amplitude, and some other production will need to make a corresponding but opposite ramp to balance the power system. These ramps can, at least partly, be predicted, but the exact time when the ramp will occur is usually hard to predict. The speed and amplitude of such ramps compared to the ramping capacity of the dispatchable production are of great interest. Rampage of wind power is discussed further by Sorensen [16].

The power system stability time horizon stretches from momentary to intra-hour balancing of power and load on the grid. The inertia of the large generators connected to the grid functions as a small energy storage that momentarily balances production and load. On the second to hour time horizon, automatic and manual frequency control handles the balancing. Traditionally, VRE has not contributed with inertia or frequency control reserves, although it is technically possible to do so at least for wind power plants [17]. For photovoltaics (PV), fast cycling energy storage to firm the power output has been suggested [18].

Energy storage can be used for balancing over all the above mentioned time horizons. The utilization of an energy storage is limited by three factors: Volume (energy), flow (power) and transmission capacity. The relation between the volume and the flow determines for how long time the storage can maintain maximum output or input. Pumped hydro storages are usually designed with storage volumes lasting one day, while the Nordic hydropower has reservoirs big enough for seasonal storage. Some rivers, for example Luleälven in Sweden, are equipped with several large turbines in parallel of which some are only operated during peak loads. However, even though there is enough volume and flow, the output can still be limited by the transmission capacity.

1.1.1 Frequency control

Power grid frequency control has been an active research area for over 50 years, and the literature on the topic is extensive. There are several surveys that provide overviews [19, 20]. Primary frequency control was mostly studied in

the 70's and 80's, using for example the root locus method [21–23], but since the 90's the research has mainly been directed towards secondary frequency control (often called load frequency control, LFC), and all sorts of control design methods have been proposed.

Robust control theory and design is well suited for power system frequency control, since the power system is a large, complex and time varying system. LFC controllers based on H_2, H_∞ and other robust methods have been designed and showed good performance also in presence of generation rate constraints, backlash and other nonlinearities [24–26], which are known to in many cases deteriorate controller performance [27]. A drawback with the classical robust control design is that it results in high order controllers which may be difficult to implement. One way to get around this problem is to use model reduction or to design a PID controller that imitates the behaviour of the high order controller. It has been shown that a PID controller designed this way for hydropower LFC can come very close to the performance and robust stability of a H_∞-controller [28].

PID controllers and their variants (PI, PI with droop, lead-lag) are the most commonly used controllers, and there is a continued research interest for LFC PID design and tuning. PID design methods using for example frequency domain specifications [28], quantitative feedback theory [29], internal model control [30], constant M-circles in the Nichols chart [31], optimal output feedback [32], and Differential Evolution [27] have been suggested for LFC applications. In recent years, many have focused on the robustness of the PI(D) controllers, for example by using specifications in the Nyquist diagram [33], Kharitonov's theorem [34] or structured singular values [35].

1.1.2 Hydropower plant dynamics

Hydropower plants are highly non-linear and complex systems, and much research effort has been put into modelling of hydropower plants with different levels of detail over the years. The amount of detail needed in the model depends on what type of phenomenon one wishes to study. To be able to study fast hydraulic transients, for example due to load rejection, models including the waterhammer effect with compressible water, elastic penstock and non-linear turbine equations are needed [36, 37]. On the electrical side, there are oscillation phenomena in the 1 Hz-range, which are modelled with the swing equation and a generator model [38]. Dynamics from surge tanks [39], shared waterways [40] and the runner angle regulation of Kaplan turbines [41, 42] may also be of importance. To be able to study more than one operational point, one needs to include the nonlinear (steady state) relation between guide vane opening and power [43–45]. For frequency control studies, when small signal amplitudes are studied and the interesting dynamics are in the range

below 0.1 Hz, a linear model of the water acceleration in the penstock is often considered enough [38].

The dynamic response of a hydropower plant can be measured and defined in different ways. Jones et al have suggested that step response, ramp response and random signal response should be used to benchmark the frequency control ability of hydropower plants [46]. Others have been more interested in testing the response to load rejection [43], [47] or the frequency response [47], [48], [49]. Step response tests are recommended by IEEE [50] to define the governor dynamics, and are used by for example the Swedish TSO in the specifications of the primary frequency control products, FCR-N and FCR-D. In Paper II, it will be argued that grid frequency step response is not the best way to test the performance of the frequency controller of a plant.

1.2 Outline of this thesis

Chapter 2 briefly presents the theoretical foundations of the research carried out in this thesis. Chapter 3 suggests a method to assess the flexibility need induced by varying renewable power, and summarises the results of Paper I. In Chapter 4, the validity of the linear hydropower plant model for frequency control studies is discussed in the light of measurement results from three Swedish hydropower plants. This chapter connects to Paper II. Chapter 5 and Paper III proposes a method to optimise the primary frequency control of the Nordic power grid within the framework of the controller structure implemented today, taking robustness, actuator work and performance into account. In Chapter 6, the conclusions of the thesis are summarized and discussed, and Chapter 7 outlines the work of the PhD thesis to come.

2. Theory

In this chapter, the theoretical foundations of this thesis are presented briefly. First, a model of the power grid, valid for small deviations from the operating point and for frequencies below 0.2 Hz, is derived. Then, a corresponding small signal analysis model of a hydropower plant is derived. These parts are based on Kundur [38]. After that, the basic concepts of system identification and robust control theory are presented. These parts are based on Ljung and Glad [51], [52].

2.1 Generator and grid

The equation of motion for a synchronous generator is

$$J\frac{d\omega_m}{dt} = T_m - T_e \tag{2.1}$$

where J [kgm^2] is the moment of inertia of the turbine and generator, ω_m [rad/s] is the mechanical rotational speed, T_m [Nm] is the driving mechanical torque and T_e [Nm] is the braking electrical torque. Defining the inertia constant H [s] as the kinetic energy at rated speed divided by the power base

$$H = \frac{1}{2}\frac{J\omega_{0m}^2}{VA_{base}} \tag{2.2}$$

and acknowledging that the torque base is $T_{base} = VA_{base}/\omega_{0m}$ and that the per unit electrical angular velocity, $\bar{\omega}_r$, is the same as the per unit mechanical angular velocity, $\bar{\omega}_m$, the per unit equation of motion of the machine is

$$2H\frac{\bar{\omega}_r}{dt} = \bar{T}_m - \bar{T}_e, \tag{2.3}$$

where the superscript bar is used to denote the normalised values. Defining a new constant $M = 2H$ (in the following, M will be referred to as the inertia of the system), and taking the Laplace transform of this equation gives

$$\bar{\omega}_r = \frac{\bar{T}_m - \bar{T}_e}{Ms}. \tag{2.4}$$

The relation between the power and frequency of a generator is

$$P = \omega_r T, \tag{2.5}$$

where P [VA] is the electrical power and T [Nm] is the torque. Small deviations from the initial values (denoted with subscript 0) can be expressed by

$$P_0 + \Delta P = (\omega_0 + \Delta\omega_r)(T_0 + \Delta T) \tag{2.6}$$

which can be approximated by

$$\Delta P = \omega_0 \Delta T + T_0 \omega_r \tag{2.7}$$

since the term $\Delta\omega_r \Delta T$ is small. The torque on the machine is the difference between the driving mechanical torque T_m and the braking electrical torque T_e, giving the equation

$$\Delta P_m - \Delta P_e = \omega_0(\Delta T_m - \Delta T_e) + (T_{m0} - T_{e0})\Delta\omega_r. \tag{2.8}$$

The last term is equal to zero, since the mechanical torque and the electrical torque are equal in steady state. The initial speed $\omega_0 = 1$ if it is expressed in per unit. This means that

$$\Delta\bar{P}_m - \Delta\bar{P}_e = \Delta\bar{T}_m - \Delta\bar{T}_e, \tag{2.9}$$

and the relation between power and frequency is the same as the relation between torque and speed, and (2.4) can be rewritten as

$$\Delta\bar{\omega}_r = \frac{\Delta\bar{P}_m - \Delta\bar{P}_e}{Ms}. \tag{2.10}$$

The change in braking electrical power is the sum of the load change,ΔP_L [VA], and the frequency dependency of the load, expressed with the load-damping constant, D,

$$\Delta\bar{P}_e = \Delta\bar{P}_L + D\bar{\omega}_r \tag{2.11}$$

which inserted in (2.10) gives

$$\Delta\bar{\omega}_r = \frac{\Delta\bar{P}_m - \Delta\bar{P}_L}{Ms + D}. \tag{2.12}$$

This equation describes the dynamics of one machine connected to a load. It is also a model of the whole power system, with all connected machines lumped into one. The crucial assumption made here is that the whole power system has the same grid frequency. This is a good approximation in the low-frequency band where the frequency control operates, but not on higher frequencies [38].

2.2 Hydropower turbine and waterways

The velocity U [m/s] of the water in the penstock of a hydropower plant is

$$U = K_u Y \sqrt{H}, \tag{2.13}$$

with guide vane opening Y [%], head H [m] and the proportionality constant K_u. Assuming small deviations, Δ, from the initial values, the change of the water velocity can be expressed as

$$\Delta U = \frac{\partial U}{\partial H}\Delta H + \frac{\partial U}{\partial Y}\Delta Y. \tag{2.14}$$

Inserting the partial derivatives and normalising the signals by their initial (steady state) values lead to the equation

$$\Delta \bar{U} = \frac{1}{2}\Delta \bar{H} + \Delta \bar{Y}. \tag{2.15}$$

The mechanical power P_m [VA] of the turbine is given by

$$P_m = K_p H U \tag{2.16}$$

with the proportionality constant K_p.

Again assuming small deviations from the initial values, the change of the normalised power is

$$\Delta \bar{P_m} = \Delta \bar{H} + \Delta \bar{U}. \tag{2.17}$$

With the expression of $\Delta \bar{H}$ in (2.15), the power is

$$\Delta \bar{P_m} = 3\Delta \bar{U} - 2\Delta \bar{Y}. \tag{2.18}$$

When the head over the turbine changes, Newton's second law of motion gives the following equation for the acceleration of the water in the penstock:

$$\rho LA\frac{d\Delta U}{dt} = -A\rho g\Delta H \tag{2.19}$$

Here ρ [kg/m^3] is the density of the water, L [m] and A [m^2] is the length and area of the conduit, g [m/s^2] is the acceleration due to gravity and t [s] is the time. The factor ρLA is the mass of the water in the conduit and $\rho g\Delta H$ is the incremental change in pressure at the turbine. The equation on normalised form becomes (by dividing both sides by $A\rho gH_0$)

$$T_w\frac{d\Delta \bar{U}}{dt} = -\Delta \bar{H} = 2\left(\Delta \bar{Y} - \Delta \bar{U}\right), \tag{2.20}$$

with

$$T_w = \frac{LU_0}{gH_0}. \tag{2.21}$$

Taking the Laplace transform of (2.20) and solving for $\Delta \bar{U}$ gives

$$\Delta \bar{U} = \frac{1}{1 + \frac{1}{2}T_w s}\Delta \bar{Y}. \tag{2.22}$$

Finally, substituting with $\Delta\bar{U}$ from (2.18) gives

$$\Delta\bar{P}_m/\Delta\bar{Y} = \frac{1 - T_w s}{1 + \frac{1}{2}T_w s} \tag{2.23}$$

This transfer function describes how the mechanical power of the turbine responds to changes in the guide vane opening of an ideal, lossless hydraulic turbine [38]. The water time constant, T_w, varies with the load.

2.3 System identification

In system identification or empirical modelling, measurements of the input and output signals of a system are used to estimate dynamical models of the system. A linear, discrete time system can be modelled by

$$A(q)y(t) = B(q)u(t) \tag{2.24}$$

where $u(t)$ is the input signal, $y(t)$ is the output signal, and A and B are polynomials in the time shift operator q, with parameters $a_1, ..., a_{na}$ and $b_1, ..., b_{nb}$ and with a time delay of nk samples. Stacking all the time shifted input and output signals and the parameters in

$$\theta = \begin{bmatrix} a_1 \\ a_2 \\ \vdots \\ a_{na} \\ b_1 \\ b_2 \\ \vdots \\ b_{nb} \end{bmatrix} \quad \text{and} \quad \varphi(t) = \begin{bmatrix} -y(t-1) \\ -y(t-2) \\ \vdots \\ -y(t-na) \\ u(t-nk) \\ u(t-nk-1) \\ \vdots \\ u(t-nk-nb+1) \end{bmatrix}, \tag{2.25}$$

the model can be written

$$\hat{y}(t) = \theta^T \varphi(t). \tag{2.26}$$

A least squares estimation of the parameter vector θ can be calculated using for example the ARX (Auto Regression eXtra input) method. In many cases when the model structure is not on the form in (2.24), a linear regression problem on the form 2.26 can still be formulated through construction of a different φ vector that could contain any combinations of $y(t)$ and $u(t)$, for example $u^2(t-1)$ or $y(t-1)u(t-2)$ [51].

2.4 Robust control

A generalised closed loop system is depicted in Figure 2.1, with the system $G(s)$ and the controller $F(s)$, consisting of one feedforward link $F_r(s)$ and

one feedback link $F_y(s)$. In many cases, for example the controllers studied in this thesis, $F_r = F_y = F$. The input signals to the system are the reference signal, $r(t)$, which is 50 Hz in our case (or zero if only the grid frequency deviation is considered); input disturbances, $w_u(t)$, which in our case is the mismatch of electricity consumption and production on the power grid; output disturbance $w(t)$, which in our case is grid frequency disturbances; and measurement noise, $n(t)$. The control signal is called $u(t)$, and is in our case the power output of the plants that operate in frequency control mode; and the physical quantity we wish to control is called $y(t)$, and is in our case the grid frequency. The closed loop system can be expressed as

$$Y = (I + GF_y)^{-1}GF_rR + (I + GF_y)^{-1}W - (I + GF_y)^{-1}GF_yN + (I + GF_y)^{-1}GW_u, \quad (2.27)$$

where I is the identity matrix and capital letter denote the Laplace transform of the signals. For simplicity, the argument of the transfer functions and signals are omitted. The equation (2.27) can also be expressed as

$$Y = G_cR + SW - TN + GS_uW_u \quad (2.28)$$

where $G_c(s)$ is the closed loop system from r to y; $S(s)$ is the sensitivity function or the transfer function from w to y; $T(s)$ is the complementary sensitivity function or the transfer function from n to y; and $S_u(s)$ is the input sensitivity function or the transfer function from w_u to u.

The control signal can be expressed as

$$U = (I + F_yG)^{-1}F_rR - (I + F_yG)^{-1}F_y(W + N) + (I + F_yG)^{-1}W_u = \\ = G_{ru}R + G_{wu}(W + N) + S_uW_u \quad (2.29)$$

with the transfer function $G_{ru}(s)$ from r to u and the transfer function $G_{wu}(s)$ from w to u.

In the context of control theory, the concept of robustness means insensitivity to model errors and disturbances. In some applications, the robustness of the controller is very important, for example due to large or unknown disturbances or uncertain or time varying system dynamics. Several methods to design robust controllers have been developed. Two of the most well known methods are called H_2 and H_∞ controller design. Both these design methods aims at minimising the transfer functions $S(s), T(s)$ and $G_{wu}(s)$ of the system, which describe the system sensitivity to model errors and disturbances. It is not possible to make all these transfer functions small on all frequencies, so part of the design method is to choose weighting functions in the frequency domain, in order to prioritise in what frequency band each of the transfer functions should be pushed down, and in what frequency band it is allowed to be larger. The H_2 design methods minimises the total energy of the weighted transfer functions (the H_2-norm), while the H_∞ design minimises the highest peaks of the weighted transfer functions (the H_∞-norm) [52].

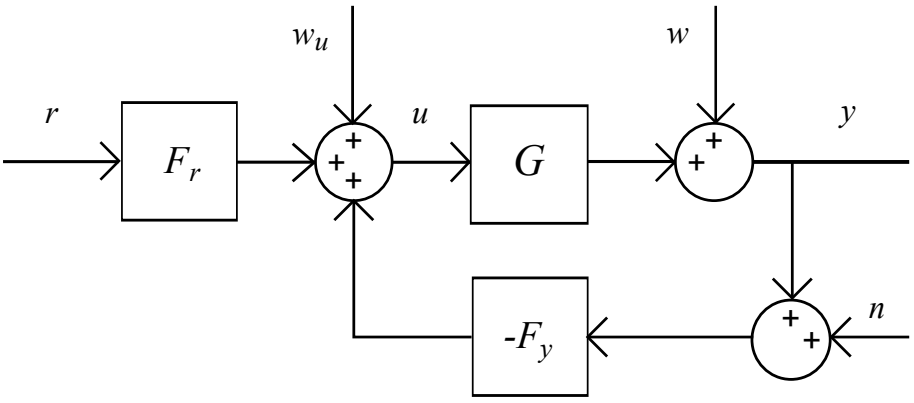

Figure 2.1. A generalised closed loop system.

2.5 PID control

Proportional-integral-derivative (PID) controllers are commonly used for control of industrial processes. In many cases, only the PI part is used, and the derivative part is set to zero. The most basic form of the PID controller is

$$U(s) = \left(K_p + \frac{K_i}{s} + K_d s \right) E(s) \tag{2.30}$$

where the control error $e(t) = r(t) - y(t)$, K_p is the proportional gain of the controller, K_i is the integration gain and K_d is the derivative gain. The inverse of K_i is often called the integration time, T_i, of the controller. However, in this thesis, T_i is used to denote the feedback time constant of the PI controller with droop which is implemented in the hydropower plants of Vattenfall, so $T_i \neq 1/K_i$. The droop limits the static gain of the controller (a PI controller has infinite static gain, due to the integration).

The derivative part of a PID controller is very sensitive to high-frequency disturbances. In general, it is therefore necessary to filter $e(t)$ before it enters the controller, or at least to filter the signal going to the derivative block.

3. Quantifying balancing need

As described in Section 1.1, the balancing need of the power system can be divided into four categories which are related to different time scales: Planning, correction and backup, rampage and stable power system [1]. In the Nordic power system, hydropower is the main resource for balancing on all four time scales. In Sweden, the power capacity of the hydropower was increased in the 1980's to be able to handle diurnal as well as seasonal load variations. The large reservoirs, located at the river sources, make it possible to save large amounts of energy from the spring and summer to the winter. This storage capacity and power capacity has a potential to balance also production from VRE. The question of how much VRE the Swedish hydropower can balance has caused a heated debate among researchers in Sweden [53]. This thesis will approach the question from another angle, and suggest a method to quantify the storage need induced by VRE over time horizons of 1-14 days, attempting to fill the gap between previous research on intra-day storage need and seasonal storage need.

3.1 Method

The power production and load of the power system has to be equal. When some of the power is produced by non-dispatchable sources (VRE), the dispatchable power needs to be equal to the net load, that is

$$P_{DISP} = P_{NL} = P_{GL} - P_{VRE}, \tag{3.1}$$

where P_{DISP} is the dispatchable power production, P_{NL} is the net load, P_{GL} is the gross load (power consumption) and P_{VRE} is the varying renewable power production. Without VRE in the system, the balancing need corresponds to the variations of the consumption or gross load. The balancing need induced by VRE can then be defined as the difference between the balancing need of the net load and the balancing need of the gross load.

The balancing need can be quantified by an energy storage measure. The basic idea of the energy storage measure is illustrated in Figure 3.1, with data from one week. In the top figure, the gross load and the net load during one week are plotted, both with their mean value subtracted. To balance this load with an energy storage, energy has to be put into storage whenever $P > 0$, and taken out of storage whenever $P < 0$. In the bottom figure, the accumulated

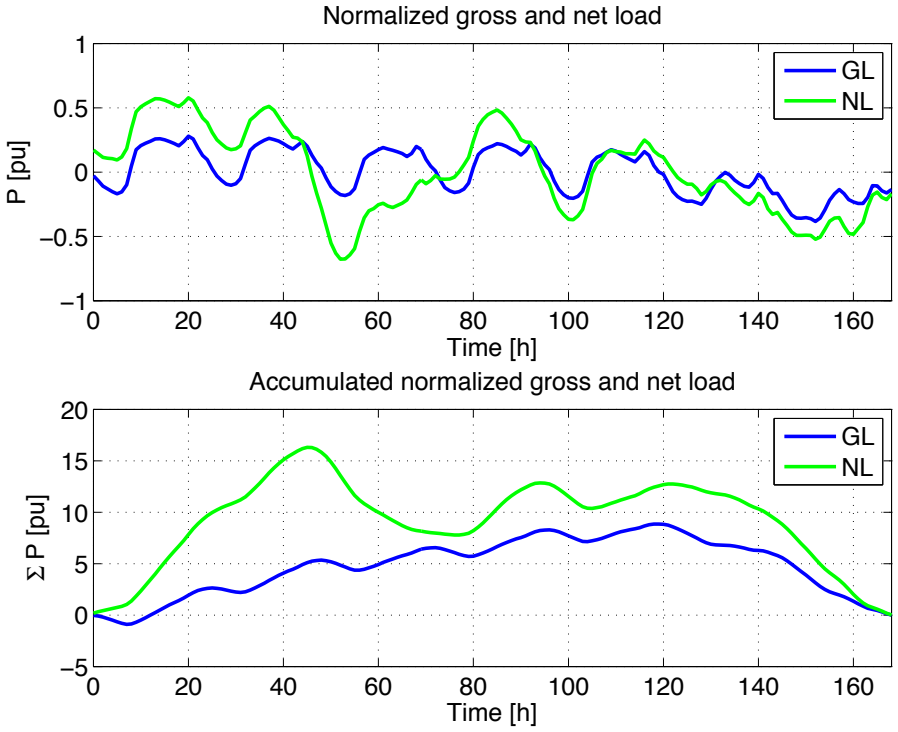

Figure 3.1. Illustration of the energy storage measure. Gross load (GL) and net load (NL) with mean values subtracted (top) and accumulated gross and net load (bottom) over one week. The difference between the largest peak and valley of the accumulated curve is the energy storage need of this week.

sum of the gross and the net load are plotted. The accumulated sum of the net load increases from t=1 to t=45, since there is surplus energy, meaning that the energy volume in the (imagined) storage is increasing. After t=45, the normalised production falls below zero and the accumulated sum starts to decrease - the stored energy volume is reduced. After a few more peaks and valleys, the curve ends up on zero, since the average power is zero (the mean value has been subtracted). Looking at the entirety of the curve, the maximal storage volume needed can be determined as the difference between the highest peak and the deepest valley, 16 pu. For the gross load, the accumulated sum starts downwards and eventually rises to 8 pu. This means that a certain energy level in the storage is needed at the beginning, and the total needed storage size is $9pu - (-1pu) = 10pu$. The storage need induced by the VRE production for this week is $16pu - 10pu = 6pu$. The same calculations can be made for all one-week periods of the year, and also for other time horizons than one week. The histogram of the storage of all periods with a certain hori-

zon during one year constitutes a statistical measure of the size of the needed energy storage. The method is described with equations in the following.

The energy storage need of the net and gross load respectively are calculated according to (3.2), with energy storage requirement S, time horizon k and load P.

$$S_k(t) = \max_{j\varepsilon[t,t+k]} \sum_{i=0}^{j} \left[P(t+i) - \sum_{n=t}^{t+k} \frac{P(n)}{k} \right] - \min_{j\varepsilon[t,t+k]} \sum_{i=0}^{j} \left[P(t+i) - \sum_{n=t}^{t+k} \frac{P(n)}{k} \right] \tag{3.2}$$

This means that for each hour (t=1:8784), a vector with the length of the time horizon k is formed [t:t+k]. The mean value of the vector is subtracted from the vector, and then the accumulated sum of the vector is calculated. The needed storage volume is considered to be the difference between the maximum and the minimum of the accumulated sum. The same operation is carried out for each hour and for each time horizon.

The cumulative distribution function F of the storage need can then be calculated as the probability of the storage need S_k being smaller than or equal to a certain value s_k:

$$F(s_k) = Pr\{S_k \leq s_k\} \tag{3.3}$$

The cumulative distribution function can be used as a measure of the firmness level. To reach a firmness level of 90%, a storage need s_k is needed such that $0.9 = F(s_k)$. The storage need at a 90% firmness level can be interpreted as the storage volume that is large enough to cover 90% of all occasions.

The above described method is applied to load data and wind and solar power production data from Germany the year 2012 (see further details in Paper I).

3.1.1 Rampage

The speed and duration of VRE production changes is also of interest, since it will put demands on the rampage capability of the balancing power plants. The rampage of VRE production can be calculated as the differenc between the production at the start and end of data samples with the same length as the investigated time horizon

$$\dot{P}_k(t) = \frac{P(t) - P(t-k)}{k} \tag{3.4}$$

with ramp speed $\dot{P}$, time horizon k and VRE power production P.

If a production forecast, $\hat{P}$, is available, part of the rampage will be known in advance, and part of the rampage will be unpredicted (due to errors in the

forecast). The ramp speed of prediction error, $\dot{e}_k$, that is the unpredicted production, can be calculated as

$$\dot{e}_k(t) = \frac{P(t) - \hat{P}(t) - \left(P(t-k) - \hat{P}(t-k)\right)}{k}. \tag{3.5}$$

Wind power production data from the wind park Horn's Rev (2009), from the entire Danish wind power (2009) and the production from photovoltaics in Germany (2011) are analysed with respect to ramp speeds. The ramp speeds are calculated with a moving window the size of the time horizon, but only the largest *not overlapping* ramp speeds are selected to form the results.

3.2 Results

The results on storage are presented in detail in Paper I, and will only be summarised here. The results on rampage are not included in the paper and will therefore be presented in detail.

3.2.1 Storage

The storage need induced by VRE increases with the time horizon and with the VRE share of the total energy production (Figure 2-4 in Paper I). The storage need *normalised with the time horizon* is approximately 20% for WP, 5% for PV and 10% for a combination of WP and PV if the energy share of VRE is 20% and the time horizon is 1-2 weeks (Table 2 in Paper I). This means that the required storage volume for a 20% share of VRE on two-week horizon is $14 \cdot 0.1 = 1.4$ times the average two-week VRE energy production. For higher shares of VRE, the storage need is approximately 30% for WP, 12% for PV and 18% for the combination of PW and WP, over time horizons of 7-50 days (Figure 5 in Paper I).

Photovoltaics has a positive impact on the power system when it comes to a one day horizon and small energy shares. With the 2012 PV share in Germany, the storage need over the one-day horizon is decreased. However, with higher shares of photovoltaics, the positive correlation of solar power and load is overshadowed by the solar variation as such, resulting in larger storage needs, especially on shorter time horizons.

Combining WP with PV mitigates the storage need since their variability have different patterns. While an integration of 80% WP would increase the storage need 6 times over a two week horizon, a combination of PV and wind increases the storage need 4 times.

The European Union has a goal that 20% of the energy supply should come from renewable sources in 2020. Wind power is expected to grow to 140-210 GW installed power in 2020 [54], with as much as 100 GW in the North Sea

region. Assuming a capacity factor of 0.3, the 100 GW wind power in the North Sea region would induce a storage need of 2.2 TWh over a 14-days horizon if the share of wind power in the receiving areas is 20%, and even more if lack of transmission makes the local share of wind power higher than that. This can be compared to the size of the entire storage capacity of the European pumped storage, which is 2.5 TWh [54]. On the other hand, seasonal reservoirs of the conventional Nordic hydropower holds 121 TWh [55], that at least partially could be used for balancing of VRE. With enough transmission capacity, this might become an important task for Nordic hydropower in the future.

3.2.2 Rampage

The worst case ramp speeds of the analysed data are presented in Table 3.1, 3.3 and 3.4. Naturally, fast ramps occur more often in the production of Horns Rev than in the more geographically distributed entire Danish wind power or the German photovoltaic production. During 2009, there are 10 occurrences when the production of Horns Rev falls with 80% of the installed power (128 MW) in one hour (Table 3.1). Ramps of shorter duration are even steeper, for example there was 10 occurrences of 15-minute ramps of more than 250%/h, that is 100 MW in 15 minutes. The ramp speed of the prediction error (Table 3.2 has equal or even higher values than the production ramp speed. The high ramp speed of the prediction error may be explained by errors in the timing of production changes. If a change in production comes earlier or later than predicted, this will give a large prediction error ramp speed.

Table 3.1. *Horns rev ramp speed in % of installed capacity per hour. Observe that when the duration of the ramp is short (e.g. 5 minutes), the ramp speed can be much higher than 100% per hour.*

Duration of ramp	**Ramp speed [%/h]**		
	1 occurrence	*5 occurrences*	*10 occurrences*
5 min	588 / -772	502 / -430	422 / -401
15 min	311 / -305	268 / -272	256 / -237
30 min	175 / -177	160 / -161	146 / -136
1 hour	93 / -95	85 / -85	82 / -80
2 hours	49 / -48	46 / -43	40 / -40
6 hours	16 / -16	15 / -16	15 / -15

For the entire Danish wind power (Table 3.3), there are 10 occurrences of ramps of approximately 15% per hour, and the fastest 1-hour ramps are 62% increase and 56% decrease. These ramp speeds are moderate compared to the ramp speeds of Horn's rev, but still considerable. Power forecast data was not available for the Danish wind power.

Table 3.2. *Horns rev prediction error, ramp speed in % of installed capacity per hour.*

Duration of ramp	Ramp speed [%/h]		
	1 occurrence	*5 occurrences*	*10 occurrences*
5 min	591 / -770	487 / -434	424 / -400
15 min	316 / -301	267 / -273	255 / -237
30 min	186 / -174	161 / -162	145 / -144
1 hour	113 / -95	86 / -89	83 / -82
2 hours	69 / -60	48 / -48	44 / -44
6 hours	22 / -22	20 / -19	17 / -16

Table 3.3. *Danish wind power ramp speed in % of installed capacity per hour.*

Duration of ramp	Ramp speed [%/h]		
	1 occurrence	*5 occurrences*	*10 occurrences*
1 hour	62 / -56	18 / -15	16 / -13
2 hours	33 / -30	16 / -13	13 / -12
6 hours	13 / -14	10 / -9	9 / -8

German solar power has smaller rampage extreme values than the Danish wind power (fastest 1-hour ramp is 29% up and 34% down), but ramps of 25-30%/h with a duration of 1-2 hours occur more often. The fast ramps of solar power are caused by sunrise and sunset as well as weather changes (cloudiness), and therefore occur more frequently than the wind power ramps which are caused by changes in the wind speed. It can also be noted from Table 3.4 that the downward ramps are generally steeper than the upward ramps, which might be explained by cloud formation during the day leading to increasing cloudiness during the afternoons.

The prediction error ramp speeds are slightly lower than the production ramp speeds for PV, especially on one hour or longer time horizons. The sunrise and sunset ought to be well known factors, improving the predictions, but the weather has a great impact on how high the midday peak will be.

Table 3.4. *German PV production ramp speed in % of installed capacity per hour.*

Duration of ramp	Ramp speed [%/h]		
	1 occurrence	*5 occurrences*	*10 occurrences*
15 min	49 / -38	37 / -33	34 / -30
30 min	33 / -36	29 / -30	28 / -29
1 hour	29 / -34	28 / -29	26 / -28
2 hours	27 / -31	26 / -27	24 / -25
6 hours	16 / -17	16 / -16	16 / -16

Table 3.5. *German PV prediction error, ramp speed in % of installed capacity per hour.*

Duration of ramp	**Ramp speed [%/h]**		
	1 occurrence	*5 occurrences*	*10 occurrences*
15 min	50 / -52	43 / -48	41 / -46
30 min	31 / -31	24 / -28	21 / -26
1 hour	16 / -29	14 / -26	13 / -25
2 hours	12 / -29	11 / -25	10 / -24
6 hours	8 / -16	6 / -16	4 / -16

4. Hydropower plant dynamics

The linear model of the hydropower plant derived in Chapter 2.2 is often used for power system analysis. As discussed in Chapter 1.1, hydropower plants can be modelled with much more detail, but due to the non-linearities of the system, the models quickly become very complex. This lead to the question of how big the error of the linear model is, what type of error it is and which part of the complex hydropower plant system that should be added to the model to improve the results the most. All this will naturally depend on what type of disturbance or what type of operation one wishes to study, and also on the properties of the individual plant. In this chapter, and in Paper II, measurements on three Swedish hydroplants are analysed in order to find in what way these plants deviate from the linear model in the specific case of frequency control operation.

4.1 Method

The dynamic behaviour of hydropower plants operating in frequency control mode was investigated through experiments on three hydropower plants in Sweden (Plant A, B and C). The plants were selected as representatives of the diverse Swedish hydropower fleet. Plant A has one diagonal turbine which is similar to a Kaplan turbine in the sense that the runner blades are adjustable. Plant B has three Francis turbines with separate intakes and a common tail race tunnel. Plant C has three Francis turbines with a common free surface tail race tunnel. More information about the plants can be found in Paper II.

A block diagram of the studied hydropower plants is given in Figure 4.1. During the experiments, a signal representing the grid frequency deviation Δf was created by a signal generator and given as input signal to the governor instead of the real grid frequency. The guide vane opening setpoint could be changed manually in a step-wise manner. The guide vane control signal, guide vane measured value and the output power were measured as well as the pressure before and after the turbine (which cannot be seen in Figure 4.1).

Three types of experiments were carried out on each plant: Grid frequency deviation sine wave with different frequency and amplitude, grid frequency deviation step changes and production setpoint step changes. All types were carried out at different loads and if possible, with different controller settings ("Ep-läge").

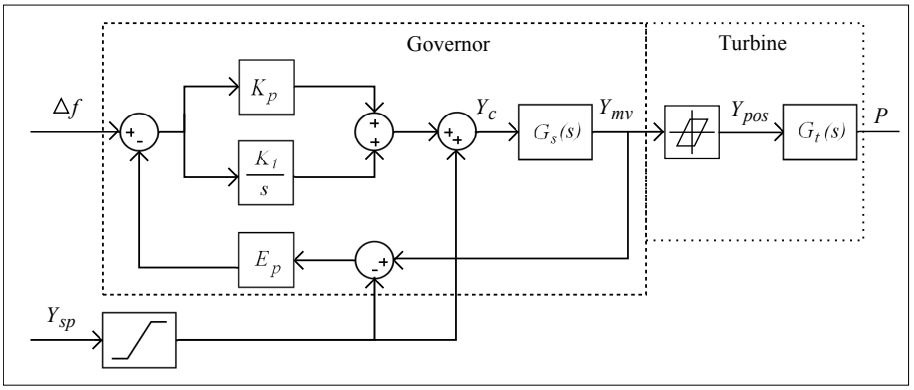

Figure 4.1. Model of governor and plant. Input signals are the frequency deviation Δf (created by a signal generator) and guide vane opening setpoint Y_{sp} (manually controlled). Output signals are the governor control signal Y_c, the guide vane measured value Y_{mv} (used as feedback signal) and the output power P.

Backlash was observed in the runner regulating mechanism of the diagonal turbine, and in the guide vane regulating mechanism of particularly the Francis turbine equipped with a guide vane regulating ring (Plant C).

As can be seen in Figure 4.1, two intermediary signals, Y_c and Y_{mv}, were measured in addition to the input signals Δf and the output signal P. Therefore it was natural to divide the model into three parts: The controller, which structure and parameters were already known; the servo $G_s(s)$ from Y_c to Y_{mv} and the rest of the plant, $G_t(s)$, from Y_{mv} to P, including turbine, waterways and generator. The servo of a hydropower plant is usually modelled by a first order lag filter [38]. Based on visual inspection of the data a time delay, T_{del}, was also included in the servo model,

$$G_s(s) = \frac{1}{T_y s + 1} e^{-sT_{del}}. \tag{4.1}$$

The main dynamics of the third part of the model, $G_t(s)$, is the acceleration of water in the penstock due to a change in the guide vane opening. A model of this was derived in Chapter 2.2 (2.23). This equation describes the system from guide vane opening to mechanical power. The dynamics of the generator is fast in comparison and can be omitted. Including a proportionality constant, K, to account for the steady state relation between guide vane opening and electrical power, the model from Y_{mv} to P at the load Y_0 is

$$G_t(s) = K \frac{-Y_0 T_w s + 1}{0.5 Y_0 T_w s + 1}. \tag{4.2}$$

This model, in the following called the PZ-model of $G_t(s)$, has a pole in the left half plane and a zero in the right half plane. The pole corresponds to the lag time constant of the model, meaning how fast it responds to any change

in the input signal. The zero in the left half plane corresponds to the model having non-minimum phase, which means that the response to any change of the input signal Y_{mv} leads to an initial response of the output signal P that is in the opposite direction compared to the final value of the response. This behaviour could be clearly seen in the step response data from Plant B and C, but not at all in the step response of Plant A. Therefore, a similar model but without the non-minimum phase behaviour (that is, without a zero in the right half plane) was also used as a comparison

$$G_t(s) = K\frac{1}{T_p s + 1}. \tag{4.3}$$

This model will in the following be called the P-model of $G_t(s)$.

Having defined the model structure of $G_t(s)$, it is straight forward to estimate the parameters K, T_w and T_p from the measured data using system identification methods. However, these models cannot adequately describe the backlash of the runner and guide vane regulating mechanisms that were observed in the data, since backlash is a non-linear (amplitude dependent) phenomenon, and the models are linear. A convenient way to include the backlash in the identification process is to model the backlash separately and pre-treat the data by running it thorough the backlash model (creating the guide vane position signal Y_{pos}) before doing the system identification (from Y_{pos} to P). The size of the backlash cannot be directly identified with this method, but if the pre-treatment and identification are repeated for different sizes of backlash, the backlash size can be determined indirectly as the one that gives the best fit to data in the estimation step.

The parameters of the model $G_t(s)$ were estimated from the measured data using the System Identification Toolbox in Matlab [56]. The estimation was carried out for both the PZ- and P-model and with different sizes of backlash. The parameters were estimated separately for each experiment (frequency sinusoid, frequency step, setpoint step and different points of operation).

4.2 Results

The main results are presented in detail in Paper II. Some additional results will be presented here, together with a summary of the main results.

4.2.1 Summarised results

In normal operation, the actuator movements demanded by the frequency controller are small, especially when the disturbances have periods of one minute or less. This means that even a small backlash will have an impact on the response of the plant. The backlash cuts off some of the amplitude of the response, and also adds to the negative phase shift. For Plant A, the phase shift

from guide vane opening to power for a disturbance with a 60 s period was $-40°$ and for Plant C it was $-17°$ in Ep2 and $-42°$ in Ep0 (see Figure 8-10 in Paper II). These numbers can be compared to the phase shift of Plant B, $-13°$, which is closer to the value expected from the linear models.

The backlash of the guide vane regulating mechanism was much smaller in the plants equipped with individual guide vane servos (Plant A and B) and larger in the plant equipped with guide vane regulating ring (Plant C).

The backlash of Plant C was well described by a backlash between the guide vane opening feedback, Y_{mv} and the turbine model $G_t(s)$. The backlash of Plant A was not situated in the guide vane but in the runner regulating mechanism. Still, the impact on the output power could be reasonably well approximated with a guide vane backlash situated before $G_t(s)$.

The diagonal turbine of Plant A did not show any non-minimum phase behaviour, and was better described by a first order lag without zero (P-model) than by the standard non-minimum phase model (PZ-model), see Figure 11 in Paper II. This can be partly explained by the slow regulation of this turbine, but there might also be other explanations.

The measured incremental gain from guide vane opening to power correspond well with tabulated values based on index-testing of the turbines (Figure 5-7 in Paper II). The incremental gain is highly depending on the point of operation, as have been showed in previous research [45]. This fact deserves to be stressed, since the praxis among many hydropower plant owners is to use the linear approximation $K \approx P_{rated}/Y_{max}$ to calculate the frequency control reserves. This method is heavily biased. For example, for Plant C, the incremental gain (and thereby the "reglerstyrka") is 30% lower than P_{rated}/Y_{max} at 80% load and 40% higher than P_{rated}/Y_{max} at 65% load.

The simplest way to decrease the impact of backlash on the frequency control would be to increase the steady state gain of the plants participating in frequency control (and correspondingly decrease the number of plants participating at a given time). The normal control actions of the participating plants would then be larger compared to the size of the backlash, and therefore the response of the plants would be closer to the response of the linear models. That is, there would be less reduction in gain from Δf to ΔP and less negative phase shift.

4.2.2 Backlash

It may sometimes be useful to have a linear approximation of non-linear backlash of hydropower plants. In this section, two different linearisations of the backlash are compared. The first one is a first order system, characterised by a time constant T_{BL} and a gain K_{BL},

$$G_{BL1} = \frac{K_{BL}}{T_{BL}s + 1}. \tag{4.4}$$

The second approximation is a time delay T_{BL} and a gain K_{BL},

$$G_{BL2} = K_{BL} e^{-sT_{BL}}. \tag{4.5}$$

The dynamic response of a backlash is highly dependent on the amplitude of the input signal. To map the behaviour, a $\pm 0.05\%$ guide vane opening backlash, modelled by the Matlab Simulink backlash block, is simulated with sinusoidal input signals of different amplitudes and frequencies, and the gain and phase of the response is calculated with the fast Fourier transform. The result is plotted in a bode-like diagram in Figure 4.2. Two models are simulated: The Vattenfall frequency controller, with parameter setting Ep0, connected to a backlash block, and the backlash block alone. In the case when the input signal first passes through the controller, the amplitude of the input signal to the backlash will vary depending on the frequency of the input signal. This means that the amplitude dependence of the backlash will be mirrored in the frequency domain (the backlash will reduce the gain and phase more on higher frequencies than it does for constant amplitude input signals). Note that even though the input signal passes through the controller, the gain and phase responses plotted in Figure 4.2 are *caused only by the backlash*. The gain and phase response of the *controller and backlash* would be even steeper.

Now, comparing the backlash gain and phase with the two approximations, using $T_{BL} = 1$ and $K_{BL} = 0.9$, it can be seen from Figure 4.3 that the two approximations give the same result for frequencies lower than 0.02 Hz. For frequencies higher than 0.2 Hz, it can be seen that although the second approximation (time delay and gain) is closer to the backlash behaviour for a constant amplitude input signal, the first approximation (pole and gain) is closer to the backlash when the input signal amplitude is affected by the controller dynamics.

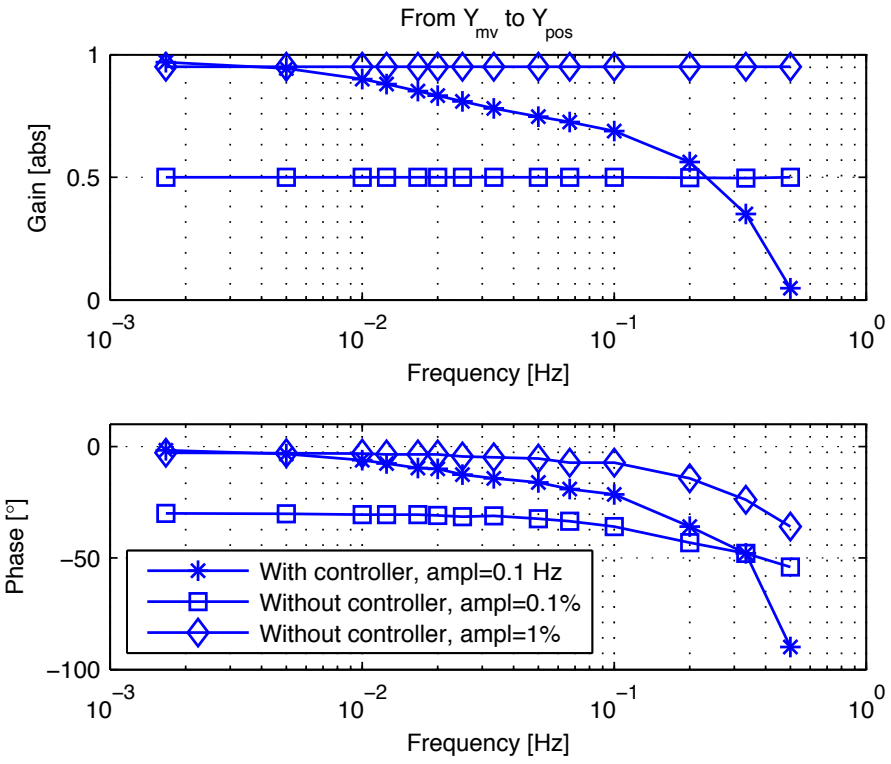

Figure 4.2. Gain and phase of the response of a $\pm 0.05\%$ guide vane opening backlash to sinusoidal input signal. Simulation of a system with the Vattenfall controller, with parameter setting Ep0, and backlash, compared to simulation of only the backlash.

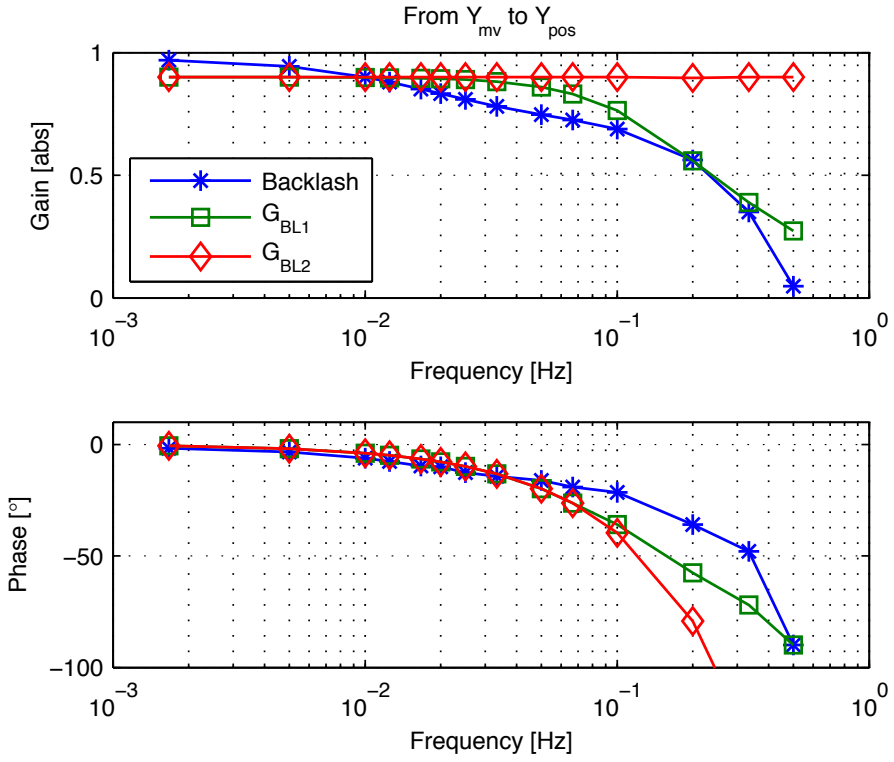

Figure 4.3. Approximations of backlash (pole and gain approximation marked with squares, time delay and gain approximation marked with diamonds), compared to a non-linear $\pm 0.05\%$ guide vane opening backlash (marked with stars). A system with the Vattenfall controller, with parameter setting Ep0, and three different backlash models are simulated with sinusoidal Δf input signal with amplitude 0.1 Hz and varying frequency.

5. Primary frequency control

In this chapter and in Paper III, a method to optimise the tuning of the primary frequency control in the Nordic grid is suggested. The method is based on ideas from robust control theory (Chapter 2.4) and the PID design methods of Åström and Hägglund [57]. The general idea is to optimise the parameters of the currently used PI controller with droop with respect to certain demands specified in frequency domain on performance, robustness and actuator work. The main contribution of this work to the research field is the discussion on how to set up these demands, and what the main trade-offs are. The power grid is complex and time varying, and there are great uncertainties in the system models and parameters. In this work, an attempt is made to take these uncertainties into account in practice.

In this chapter, and in Paper III, a control theory oriented notation is used instead of the physical quantity oriented notation in the other chapters. The notation is explained in Table 5.1. In this chapter, the signals are treated in pu, while in Chapter 4, they were treated in their physical units.

5.1 The Nordic power grid

The Nordic power system is dominated by hydropower, and frequency control is almost entirely carried out by hydropower plants. The transmission system operators (TSO) buy frequency control products from the plant owners. There are two products for primary frequency control (or frequency containment reserve): FCR-N for normal operation ($49.9 < f < 50.1$ Hz) and FCR-D for disturbed operation ($f < 49.9$ Hz). The technical specifications for the two reserves are defined in different ways in the different Nordic countries. In Sweden, the guideline is that FCR-N reserves should be committed to 63% within 60 seconds, while FCR-D reserves should be committed to 50% within 5 seconds. In addition to the primary frequency control, there is a manually operated secondary control (FRR-m), and since 2013, an automatic secondary control (LFC, FRR-a) has been tested and is currently in operation during a few hours per day. In this thesis, the primary frequency control for normal operation, FCR-N, is analysed.

The Nordic power grid can be seen as the single-input single-output (SISO) system, depicted in Figure 5.1. The system is lumped into one rotating mass and one hydropower plant controlling the frequency of the system. Electromechanical oscillations between one generator and the grid and inter-area

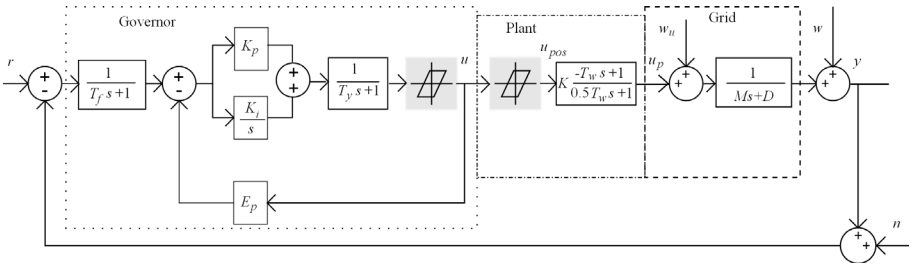

Figure 5.1. Model of the Nordic power system, with all power plants lumped into one. In the model used for controller design, the two grey backlash blocks are omitted. In the model used for evaluating control performance, they are included. Signals and parameters are explained in Table 5.1 and Table 5.3.

oscillations are not modelled explicitly, but handled as grid frequency disturbances w. This approximation is reasonable since the unmodelled dynamics are present in a higher frequency band than the dynamics of the grid frequency control [38]. The main disturbance of the system is load disturbance w_u. Load disturbance can arise both from changes in the load and changes in the power production. The sign of the load disturbance is chosen so that if more power is added to the system (increase of generation, decrease of load), the sign is positive. The signals of the system and their abbreviations are explained in Table 5.1. All signals are scaled to per unit with the bases given in Table 5.2. The power base is not chosen as the typical total load of the system, but instead as the total power of the plants participating in FCR-N, if they all operate with 10% droop ($E_p = 0.1$). This base is chosen to simplify comparison with one plant operating with the Vattenfall controller setting Ep0.

Table 5.1. *Definitions of the signals in Figure 5.1. The corresponding notation of Chapter 4 is also specified. Note that in this chapter, the signals are treated in pu, while in Chapter 4, they were treated in their physical units.*

Signal	Ch.4	Physical variable	Physical unit
r		Grid frequency deviation reference (=0)	Hz
y	Δf	Grid frequency deviation from 50 Hz	Hz
u	ΔY_{mv}	Plant control signal, guide vane opening dev.	%
u_{pos}	ΔY_{pos}	Plant guide vane opening position dev.	%
u_p	ΔP	Plant output power deviation	MW
w_u		Load disturbance (Positive if power is added)	MW
w		Grid frequency disturbance	Hz
n		Measurement disturbance	Hz

The governor is modelled as a first order low-pass input signal filter, a PI controller with droop and a first order lag representing the hydraulic guide vane servo

$$C(s) = \frac{K_p s + K_i}{(T_f s + 1)(T_y s^2 + (E_p K_p + 1)s + E_p K_i}. \tag{5.1}$$

Table 5.2. *Per unit bases used in this chapter.*

Type	Value	Applies to signal
P_{base}	37650 MW	u_p, w_u
f_{base}	50 Hz	r, y, w, n
Y_{base}	100%	u, u_{pos}

This controller structure is implemented in the hydropower plants owned by Vattenfall Vattenkraft AB, the largest hydropower owner in Sweden. Although the controller structure varies among the generating companies, their functionality can in most cases be translated into this structure. It should be noticed that this controller uses guide vane opening feedback and not power feedback, and that this is the most common case in Nordic hydropower plants.

A backlash or floating deadband is also included in the governor model. Sometimes a floating deadband is included in the controller in order to decrease small movements and wear on the turbine and actuator. In most Nordic hydropower plants, no such deadband is implemented.

The hydropower plant and power grid are modelled with a standard linear model [38], but including a guide vane opening backlash in the hydropower plant and an uncertain gain, K, from guide vane opening to output power, motivated by the use of guide vane opening feedback in the controller. The gain of a plant varies with the operational point, and in practice the total gain is calculated in advance, in order to commit the right number of plants to frequency control during each operational hour. There is however a considerable uncertainty in the total gain. As was showed in Paper II, the power output can be affected by backlash in the guide vane regulating mechanism. Therefore a guide vane opening backlash is included in the model.

The system parameters are listed in Table 5.3 with a nominal, minimum and maximum value. The values for inertia, M, and frequency dependence of the load, D, are based on personally communicated estimations by the Swedish TSO. The water time constant, T_w, is based on typical values for hydropower plants owned by Vattenfall. The servo time constant, T_y, is based on the measurements described in Paper II, and the maximal value is set rather high in order to implicitly include some of the effect of backlash in the uncertainty of the linear part of the model. The standard setting of the controller parameters used in Vattenfall plants, called "Ep0", is used as nominal controller parameters.

5.2 Method

A linear model (Figure 5.1 but with the shaded backlash blocks omitted) is used for controller design, and a non-linear model (all of Figure 5.1) is used for evaluation of the performance of the optimised controllers by simulation.

Table 5.3. *System and controller parameters presented with nominal, minimal and maximal values in per unit (and in physical units in parenthesis).*

Parameter	Nominal	Min	Max	Unit
System parameters				
M	13 (250)	8 (150)	24 (450)	s (GWs)
D	0.5 (360)	0.4 (300)	1 (750)	pu/pu (MW/Hz)
T_w	1.5	0.5	2	s
K	1 (37.65)	0.9 (34)	1.1 (41)	pu/pu (GW/%)
T_y	0.2	0.1	1	s
Controller parameters (Nominal values, "Ep0")				
K_p	1			pu
K_i	1/6			s^{-1}
E_p	0.1			pu
T_f	1			s
$1/E_p$	10 (7530)			pu/pu (MW/Hz)
$T_i = 1/(E_p K_i)$	60			s

The linear model used for controller design can be characterised by the transfer functions from the input signals n, w_u and w to the output signals u, u_p and y. The approach of robust controller design taken here is to make a weighted minimisation of these transfer functions in frequency domain [52].

The Matlab Robust Control Toolbox [58] is used to define the system, set up weighting functions and optimise the controller parameters. The weighting functions are expressed as soft and hard tuning goals, which are translated into normalised functions $f_i(x)$ (soft) and $g_i(x)$ (hard) by the software which then solves the minimisation problem

$$\text{Minimise } \max_i f_i(x) \text{ subject to } \max_j g_j(x) < 1, \quad x_{min} < x < x_{max} \tag{5.2}$$

with

$$f_i(x) = \| W_i(s)^{-1} G_i(s,x) \|_\infty \tag{5.3}$$

$$g_i(x) = \| W_i(s)^{-1} G_i(s,x) \|_\infty, \tag{5.4}$$

where the user-defined optimisation objectives $W_i(s)$ are the maximal gains of the closed loop transfer functions $G_i(s,x)$ with the parameter values x.

The tuning goals are described in subsections 5.2.1-5.2.4 and plotted in Figure 2 in Paper III.

The following optimisation constraints on parameters were used:$K_p > 0$, $T_i > 0, E_p > 0.1$. The constraint on E_p means that the total amount of FCR-N in the system cannot be increased.

5.2.1 Disturbance suppression - $G_{w_u y}(s)$

The main goal of the controller is to attenuate load disturbances w_u, which means that the transfer function $G_{w_u y}$ from load disturbance w_u to grid frequency y should be minimised. First of all, small steady state error is required. Today, the Nordic TSO:s aim at a fixed amount (753 MW) of regulating power participating in primary frequency control in the grid frequency band 49.9-50.1 Hz. This corresponds to a steady state gain from w_u to y slightly below 0.1 pu/pu. The different TSO:s have slightly different demands on activation time. In Sweden, the reserve should be activated to 63% after 60 seconds. To keep the low-frequency performance of today, a low frequency tuning goal of 0.1 pu/pu maximal gain (hard from 0 to 0.000167 Hz and soft from 0.000167 Hz to 0.00167 Hz) for G_{wuy} is used in the optimisation. Further, it is desired to minimise the peak gain of $G_{w_u y}$. This is expressed as a soft tuning goal $\| G_{w_u y}(i\omega) \|_\infty < 0.5$ pu/pu.

5.2.2 Model uncertainty - $T(s)$

The transfer function from measurement noise n to output signal y is called the complementary sensitivity function $T(s)$. The system robustness to model errors is connected to $T(s)$ [52]. Given a true system $G_0 = (I + \Delta_G)G$ with the model G and the model error Δ_G, where G and G_0 has the same number of unstable poles, the true system is stable if

$$|T(i\omega)| < \frac{1}{|\Delta_G(i\omega)|}. \tag{5.5}$$

The model uncertainties given in Table 5.3 can be expressed as a set of transfer functions $\Delta_{G_i}(i\omega)$. The minimum of $1/\Delta_{G_i}(i\omega)$ is used as a hard tuning goal for maximal gain of $T(i\omega)$.

5.2.3 Sensitivity - $S(s)$

The transfer function from grid frequency disturbance w to grid frequency y is called the sensitivity function $S(s)$, and describes how a relative model error is transformed to an error on the output signal [52]. The peak of the sensitivity function is also a result of the distance from the Nyquist curve of the open loop system to the point (-1,j0), and determines how damped or oscillatory the step response of the system is. The hard tuning goal $\| S(i\omega) \|_\infty < 1.7$ pu/pu is used in the optimisation. This value is based on based on visual inspection of the system step response. Further discussion of sensitivity margins can be found in the literature [57].

5.2.4 Control signal restriction - $G_{wu}(s)$

There are two reasons to limit the high frequency content of the control signal. First of all, there are unmodelled electromechanical dynamics in the high frequency band (>0.2 Hz) [59] which will act as a disturbance w on the system. Limiting the transfer function G_{wu}, from w to u, makes sure that the controller mostly will ignore these disturbances. Secondly, control actions cause wear on the turbines and actuators. The wear is believed to be correlated to the travelled distance of the actuator and the direction changes. This also makes restriction of the high frequency gain of G_{wu} desirable. Based on this reasoning, a high frequency tuning goal of 1 pu/pu maximal gain (soft from 0.2 Hz to 0.5 Hz and hard from 0.5 Hz to infinity) for G_{wu} is used in the optimisation. This will also indirectly limit the gain from measurement noise n and load disturbance w_u to u.

5.2.5 Optimisation cases

Three optimisation cases are chosen, in order to put some light on the most important trade-offs in the design:

C1) All the tuning goals described in the previous section are applied.

C2) The G_{wu} tuning goals are not applied. This case is constructed to illustrate the trade-off between performance and disturbance sensitivity of the control signal.

C3) The $G_{w_u y}$ low-frequency gain tuning goal is increased from 0.1 pu/pu to 0.2 pu/pu. This case is constructed to illustrate the trade-off between low-frequency and mid-range frequency disturbance suppression.

The controllers C1-C3 are evaluated in frequency domain in Figure 2 in Paper III.

Further, the controller C1 is re-optimised for a system with one system parameter at the time changed to its extreme value. The purpose is to describe how each system parameter influences the optimal controller tuning. The results are presented in Figure 5 and Table 6 in Paper III.

Finally, the system is expanded to include three hydropower plants with different characteristics, instead of one lumped plant. The controller parameters of each plant is optimised in this system, and compared to the parameters optimised for the one-plant system. The purpose is to check the feasibility of controller optimisation on the simplified one-plant system. The results are presented in Figure 6 and Table 7 in Paper III.

5.2.6 Evaluation of controller performance

The performance of the optimised controllers can also be evaluated by simulation of the non-linear system in Figure 5.1, including backlash. In the literature, the controller performance is most often evaluated by simulation of a

load step disturbance [30,32,50,60]. This type of evaluation is reasonable if the purpose of the controller primarily is to handle larger disturbances, such as loss of a power line or a production unit. However, the purpose of the frequency control analysed in this thesis, FCR-N, is to handle normal operation without large disturbances, and typical load variations would be a better input signal in evaluation of its performance. Unfortunately, there is no continuous measurement of the total load of the grid available. The grid frequency is measured, but any calculation of the load disturbance from the grid frequency presupposes a model of the system, which is uncertain. Therefore, to imitate normal operation, the system model is simulated with white noise with standard deviation 0.0035 pu as load disturbance input signal. The standard deviation of the white noise is chosen to give a frequency standard deviation with the Ep0-controller that is the same order of magnitude as the real grid frequency standard deviation.

The performance of the controllers is quantified with the standard deviation of the grid frequency, the travelled distance of the actuator (corresponding to the signal u) and the guide vanes (corresponding to the signal u_{pos}), and the number of direction changes of the actuator and the guide vanes. The result is presented in Table 5 and Figure 3 in Paper III.

5.3 Results

The main results are presented in detail in Paper III. Some additional results will be presented here, together with a summary of the main results.

5.3.1 Optimisation with reduced uncertainty

The robustness demands on the complementary sensitivity function $T(s)$ of the system has great impact on the controller optimisation. In the analysis in Paper III, the tuning goal for $T(s)$ is kept the same in all optimisation cases, in order to get consistent comparisons, for example to the three-plant system. However, one might also ask what happens to the optimisation result if the uncertainties of the system parameters are decreased (for example by more measurements or further analysis of already available data).

To assess the impact of model uncertainty on the optimisation, the controller is optimised for systems where the uncertainty of one system parameter at the time is reduced. If for example the system inertia could be measured or estimated with good accuracy, it may be possible to differentiate between low-inertia and high-inertia periods and to reduce uncertainty. In Table 5.4, the system parameters are changed to the mid point of the downward and upward original uncertainty interval, and the uncertainty interval is reduced to be only the downward, only the upward or half the interval. Looking at the result for optimisation with the nominal parameter value ($M = 13$, $D = 0.5$,

$T_w = 1.5$, $K = 1$) but decreased uncertainty interval, compared to the optimisation with nominal system parameters and the original uncertainty interval (first line in the table), it can be seen that the uncertainty pushes the controller in a conservative direction. For example, for $M = 13$, with the original uncertainty interval $K_p = 2$ and $T_i = 56$, while for $M = 13$ with reduced uncertainty interval, $K_p = 2.3$ and $T_i = 49$. However, also with the reduced uncertainty intervals, the optimisation leads to a conservative controller for the low inertia system and a more aggressive controller for the high inertia system. The other requirements (limited $S(s)$ and $G_{wu}(s)$) are still limiting the achievable performance.

Table 5.4. *Controller parameters optimised for different values of the system parameters and reduced uncertainty.*

Varied parameter	**Uncertainty interval**	**Optimised parameters**			
		K_p	T_i [s]	E_p	T_f[s]
Nominal		2	56	0.1	0.83
M =10	8 - 13	2	63	0.1	0.78
M =13	10.5 - 18.5	2.3	49	0.1	1.1
M =19	13 - 24	2.8	36	0.1	1.4
D =0.45	0.4 - 0.5	2.2	54	0.1	0.93
D =0.5	0.45 - 0.75	2.1	53	0.1	0.91
D =0.75	0.5 - 1	2.3	42	0.1	1.2
T_w =1	0.5 - 1.5	2.5	37	0.1	1.3
T_w =1.5	1 - 1.75	2.3	49	0.1	1.1
T_w =1.75	1.5 - 2	2.2	57	0.1	0.89
K =0.95	0.9 - 1	2.1	41	0.1	0.36
K =1	0.95 - 1.05	2.2	52	0.1	0.96
K =1.05	1 - 1.1	2.1	56	0.1	0.98

5.3.2 Summarised results

All the optimisation cases results in controllers with larger proportional part, K_p, than the Ep0-controller. It is also clear that the optimal tuning of the controller is highly dependent on the inertia of the system. With a high inertia, the primary control can be more aggressively tuned (higher K_p and shorter feedback time constant T_i), and with a low inertia the tuning needs to be less aggressive. Since the inertia of the grid varies with the type and number of synchronised power plants, it could be beneficial to use a gain scheduling approach with different parameter settings depending on the current inertia of the grid. The inertia depends on the number of synchronised generators and their type and size, which means that the TSO has an approximate knowledge of how this parameter varies over time. To produce an accurate, on-line approximation of the inertia, however, might be challenging.

The optimisation shows that from the point of view of the grid, the primary control should be tuned more conservatively if the water time constants of the plants are long. Ideally, the whole system should be optimised globally, but this is impractical due to the vast number of plants that participate in primary frequency control. Comparing the result from tuning one plant at the time under the assumption that it alone provides primary control for the system does gives similar results as a global optimisation of all plants. Since different plants participate in frequency control at different times, it is also reasonable to use a parameter setting that can work well independently of the other plants. Taking that into account, it is reasonable to optimise each plant separately.

The conclusions about how the controllers should be tuned for different system parameters are highly dependent on the demands on the sensitivity functions $T(s)$ and $S(s)$ and on G_{wu} (limiting the high frequency content of the control signal). If performance was prioritised over robustness and disturbance insensitivity, the conclusion might be that a faster controller is needed if the inertia is low or the water time constant is high.

There are some trade-offs to consider. First of all, demanding a small steady state and low-frequency grid frequency error limits the possibility to achieve good performance in the mid-frequency range, at least if it is combined with demands on low disturbance sensitivity of the control signal on high frequencies. The demand on low-frequency disturbance suppression is a somewhat open question, since there are other types of control that might take on this task. Maybe the normal reserve (FCR-N) could focus on mid-frequency range disturbance suppression, and secondary control (FRR-A, LFC) could handle the persistent load deviations. Such a solution needs to be further studied before anything can be concluded about its feasibility.

Demands on low disturbance sensitivity of the control signal in the high frequency range greatly limits the performance. The demands are set conservatively in this thesis, since the high frequency behaviour of the power grid is not included in the model. It is clear, however, that the performance can be improved if higher sensitivity can be allowed, that is, if it can be showed that there is no risk for unwanted interaction with inter-area oscillations and other phenomena in frequency range above 0.2 Hz. The draw-back is that it would also most likely increase the wear on the turbines and actuators of the controlling plants.

There is a clear trade-off between actuator work and performance. Simulation of a white noise load disturbance showed that while the grid frequency deviation decreased with the optimised controller, the actuator work increased. However, with a small floating deadband in the controller, the actuator work could be considerably decreased while keeping some of the improved performance. Since there is already some backlash in the actuator of most plants, allowing a small backlash in the controller seems reasonable. However, there is always a risk in introducing non-linearities in the system. No limit cycle oscillation due to backlash can be seen in the simulations of the non-linear

system, but the margins to limit cycle oscillations could be further analysed with for example the describing function method.

It can be concluded that the grid frequency quality can be much improved, especially in the 40-90 s band, by retuning of the currently used primary frequency controllers. The robustness of the system can be improved at the same time.

6. Conclusions

The aim of this thesis has been to develop research results that are practically applicable for the Nordic grid transmission operators and hydropower industry. I will therefore venture to draw some conclusions and make some recommendations, that I hope can be useful:

The proportional part of the controller is important. Increasing the proportional part of the PI controller improves the timing (or phase shift) of the response. A good balance between the proportional and integral part of the controller is crucial for a good controller performance. Today, the proportional part is set lower than what is optimal, at least in the investigated Vattenfall plants. If the droop (E_p) of the plant is changed, the other controller parameters (K_p and K_i) also have to be changed if the same dynamic performance should be achieved (so that one plant operating with low droop is interchangeable with two or several plants operating with higher droop).

Avoid high droop (low static gain or "reglerstyrka"). Hydropower plants can be expected to have some backlash in the guide vane regulating mechanism (and in the case of Kaplan turbines, in the runner regulating mechanism). If the static gain of the controller is low (typically 20%/Hz), the dynamic response to disturbances with periods of approximately one minute will be very small, which means that even a small backlash (typically 0.1-0.3% will have a considerable impact on the amplitude and phase of the response. With a higher static gain, the dynamic gain will also be higher and the backlash will have less impact on the response. Therefore it is preferable to distribute the control task on fewer plants, operating with lower droop, compared to distributing the control task on many plants operating with higher droop.

The quota P_{rated}/Y_{max} is not a good approximation of the incremental gain. The incremental gain of a plant in frequency control mode, measured in MW/Hz, is highly dependent on the operating point of the plant. The approximation that the power is proportional to the guide vane opening can lead to considerable over- or under-estimation of the static gain ("reglerstyrka"). This has been shown before [45], but deserves to be stressed since this approximation is often used by the hydropower plant owners. Instead, the incremental gain can be calculated from data collected from index tests of the turbine. The results of Paper II shows that for the investigated plants, the incremental gain calculated from index test data corresponded well to the incremental gain measured at frequency control tests of the plants.

Sinusoidal input signals are recommended for frequency control testing. Experiments with a sinusoidal grid frequency input signal of varying frequencies gives relevant information of the backlash of the system as well as the linear dynamics. The impact from surge on the plant response can also be investigated through such measurements. Grid frequency step response tests, which are recommended by IEEE [50], give some information about the dynamics of the plant, but mostly in the low-frequency range. It is important to note that amplitude dependent dynamics (such as backlash) might be important for the normal behaviour of the plant, and therefore it is important to make tests with both small and larger amplitudes.

There is a trade-off between the performance of the frequency control in the low-frequency range and the mid-frequency range. Demands on high disturbance suppression at low frequencies limit the performance at mid-range frequencies, at least if combined with demands on limited high frequency control signals and limited sensitivity functions.

There is a trade-off between actuator work and frequency control performance. Limiting the high frequency content of the control signal affects the mid-range disturbance suppression.

Low system inertia calls for a slower controller. Given the demands on on robustness and sensitivity discussed in Paper III, a conservative tuning of the primary control is better for a system with low inertia, while a more aggressive tuning is preferable for a system with high inertia. However, the disturbance suppression is not as high for the low inertia system with the conservative controller tuning. If high mid-range disturbance suppression is prioritized over robustness and disturbance insensitivity, one might come to the opposite conclusion, that low inertia calls for a faster controller.

Slow plants call for slower controllers. From a system perspective, a conservative tuning of the primary control is suited for plants with long water time constant. Just like the conclusion about inertia above, this conclusion depends on the demands on system robustness and disturbance sensitivity discussed in Paper III.

Balancing VRE production over weeks and months may become more challenging than the intra-day and intra-hour balancing. With high shares of VRE in the energy mix, the energy storage need is approximately 20% times the time horizon (for a mix of wind power and photovoltaics). To manage long periods of low or high VRE production, very large storage volumes are needed. The seasonal reservoirs of the Nordic hydropower constitutes such large energy storages, and could play an important role in balancing the future power grid, over short *and* long time horizons. Flexible operation of thermal power plants, like gas turbines, or demand side management may also be a part of the solution.

7. Future work

The research of this thesis has been focused on primary frequency control. The next step is to include the secondary frequency control (LFC) in the analysis. One central topic is the interaction between primary control and LFC. There is a concern that the division into two different control schemes leads to double work, so that each disturbance is balanced twice, first by the primary control and then by the LFC which attempts to restore the primary control reserves. Can the two control schemes be coordinated or in some other way adjusted so that double work is avoided? And how should each control system be tuned to achieve the best overall performance?

I would also like to address the more general question of advantages and drawbacks with different types of LFC controllers. What can be gained from using additional input signals to the LFC controller, such as scheduled changes in the load on HVDC cables or other known or predicted load or production changes? What can be gained from more advanced LFC controllers in general, for example model predictive control, MPC?

In the research on primary frequency control, I have so far used a simplified model of the power grid, in which electromechanical oscillations are omitted. In the continuation of my research, I would like to include more power system dynamics in the model, at least the major inter-area oscillations of the Nordic power system. With a widened frequency range of the model, it would be interesting to benchmark a controller with derivative part (PID or lead-lag) with the PI controller suggested in Paper III. What is the gain and what is the cost with a more aggressive frequency control? With the strict demands on disturbance sensitivity used in Paper III, a derivative part does not significantly improve the controller performance. However, if these demands are softened, the result might be somewhat different.

Another related topic is the question of how harmful different types of control actions are to the turbine and actuator, and how to design control strategies that minimises wear. In my research so far, the number of direction changes of the actuator and guide vanes and the total distance travelled by the actuator and guide vanes have been used as measures of the wear. With a more extensive model of the hydropower plant or with results from other studies, it might be possible to improve the measures of wear and to use them explicitly in control design. This work will be done in cooperation with other researchers.

8. Summary of papers

Paper I

Power system flexibility need induced by wind and solar power intermittency on time scales of 1-14 days. This paper describes a method to assess the needed production flexibility to adapt the power system to the production from varying renewable energy sources such as wind power and photovoltaics over time horizons of 1-14 days. Load and production data from the German power system is used to quantify the flexibility need in terms of power and energy storage requirement due to higher shares of renewable energy (20-80%).

I performed the analysis and wrote the paper. N. Dahlbäck came up with the idea of the method.

The paper was submitted to Renewable Energy in July 2014.

Paper II

Field measurements and system identification of three frequency controlling hydropower plants. The dynamic behaviour of hydropower plants participating in primary frequency control is investigated in this paper through frequency response, step response and setpoint change tests on three Swedish hydropower plants. Grey-box system identification is used to estimate the parameters of simple linear models suitable for power system analysis and the major shortcomings of the linear models are discussed.

I performed the major part of the analysis and wrote the paper. P. Norrlund contributed with suggestions to the analysis, quantification of the backlash, theoretical calculations (based on drawings) of the water time constants and surge periods and calculation of the polynomial that is called "tabulated incremental gain" in the paper. The field measurements were planned and performed by P. Norrlund and Gothia Power, with some smaller contribution from me.

The paper was submitted to IEEE Transactions on Energy Conversion in September 2014.

Paper III

Robust primary frequency control in a system dominated by hydropower. In this paper, the parameters of the primary frequency controller currently used in the Nordic power system are optimised using a robust control approach. The trade-off between performance, actuator work and robustness is analysed in frequency domain and time domain, and the sensitivity to disturbances and model errors is discussed.

I performed the analysis and wrote the paper.

The paper was submitted to Control Engineering Practice in November 2014.

9. Acknowledgements

The research presented in this thesis was carried out as a part of "Swedish Hydropower Centre - SVC". SVC has been established by the Swedish Energy Agency, Elforsk and Svenska Kraftnät together with Luleå University of Technology, KTH Royal Institute of Technology, Chalmers University of Technology and Uppsala University.

Participating companies and industry associations are: Alstom Hydro Sweden, Andritz Hydro, E.ON Vattenkraft Sverige, Falu Energi & Vatten, Fortum Generation, Holmen Energi, Jämtkraft, Jönköping Energi, Karlstads Energi, Mälarenergi, Norconsult, Skellefteå Kraft, Sollefteåforsens, Statkraft Sverige, Sweco Energuide, Sweco Infrastructure, SveMin, Umeå Energi, Vattenfall Research and Development, Vattenfall Vattenkraft, Voith Hydro, WSP Sverige and ÅF Industry.

I would like to express my gratitude to some persons who have been important to this licentiate project. First of all my supervisors at Uppsala Universtity: Urban Lundin, Per Norrlund and Bengt Carlsson, thank you for for your support and for valuable discussions. Thanks to colleagues at Vattenfall: Niklas Dahlbäck and Erik Spiegelberg, for sharing your knowledge and ideas. Jonas Funkquist and Katarina Boman, for teaching me everything I know about modelling and control (prior to this project) and for being such good mentors. Johan Bladh, for opening the path for me into the area of hydropower and frequency control in the first place, and for your support ever since. Karin Ifwer, Jonas Persson, Reinhard Kaisinger, Roger Hugosson, Harald Boman and the operators at Voullerim DC for taking an interest in this project and for helping me along. To Evert Angeholm and his colleagues at Gothia Power for measurements and data. To the SVC reference group, for supporting this project with your knowledge. Thanks also to my fellow hydropower PhD students at Uppsala University: Birger Marcusson, Weijia Yang, José Pérez, Jonas Nøland and Mattias Wallin, for sharing the everyday ups and downs. And last but not least, to my girlfriend Tove Solander, for love and support and for making sure that I do not get too preoccupied by work.

10. Svensk sammanfattning

Produktionen och konsumtionen av elektricitet måste alltid vara i balans på elnätet. En liten energimängd finns lagrad som rotationsenergi i de tunga maskiner som är direktkopplade till elnätet, framför allt vattenkraftens och kärnkraftens generatorer och turbiner, men den motsvarar bara några sekunders förbrukning. Om produktionen är lägre än konsumtionen så lånas energi från den roterande massan, vilket innebär att maskinerna roterar långsammare och långsammare. Denna rotationshastighet motsvarar också frekvensen på elnätets spänning och ström, vilket innebär att den elektriska frekvensen i hela nätet sjunker. Vattenkraftverken mäter frekvensen och ökar sin produktion om frekvensen sjunker, eller minskar sin produktion om frekvensen stiger. Detta kallas frekvensreglering. Alltför låg frekvens kan medföra haverier i termiska kraftverk, vars långa axlar kan hamna i resonans och skjuvas av. Frekvensregleringens mål är att hålla frekvensen nära 50 Hz, det vill säga se till att produktionen balanserar konsumtionen, även vid stora störningar. Frekvenskvaliteten på det Nordiska elnätet har försämrats under de senaste 20 åren. Det kan finnas många olika förklaringar till detta, exempelvis avregleringen av elmarknaden, ökningen av varierande förnybar produktion och en gradvis förändring av hur frekvensregleringen körs. Man har också lagt märke till en svävning i nätfrekvensen med periodtiden 40-90 sekunder, vars amplitud tycks öka. Det finns också farhågor från vattenkraftsägarna om att slitaget på vattenkraftturbinerna har ökat, kanske på grund av en ökad frekvensreglering.

Den här avhandlingen består av tre delstudier. Den första delstudien beskriver hur behovet av balansering över långa tidshorisonter (1-2 veckor) påverkas av en ökad andel sol- och vindkraft. De andra två delarna handlar om balansering inom drifttimmen, närmare bestämt frekvensreglering.

Delstudien om balanseringsbehov utgår från ett energilagringsperspektiv. Behovet av energilagring definieras här som integralen av nettolastens avvikelse från genomsnittet. Produktions- och lastdata från det tyska elnätet skalas upp och används för att beräkna energilagringsbehovet över olika tidshorisonter och för olika mängd sol- och vindkraft (varierande förnybar energi,VRE) i systemet. Resultaten visar att med 20 energiprocent VRE så behöver man lagra ungefär 10% av den typiska tvåveckorsproduktionen för att klara balansen över tvåveckorshorisonten. Om VRE dominerar energiproduktionen så närmar man sig lagringsbehovet 20%. Långa perioder med svaga vindar och lite sol kan bli en utmaning för kraftsystemet i framtiden, eftersom stora energimängder krävs för att klara balansering över långa tidhorisonter.

Delstudierna om frekvensreglering tar avstamp i systemet som det ser ut idag, med avsikt att försöka hitta enkla förbättringsåtgärder som kan ge betydande resultat. En gyllene regel inom reglertekniken är att testa enkla lösningar först, eftersom det har visat sig att rätt intrimmade enkla regulatorer ofta kan ge nog så bra resultat som mer avancerade regulatorer i många typer av system.

Genom experiment på tre svenska vattenkraftverk och analys av mätresultaten undersöks hur bra enkla, linjära modeller kan beskriva dynamiken i ett vattenkraftverk, och vilka som är de viktigaste avvikelserna som på något sätt bör inkluderas i modellen. Resultaten visar att glapp i ledskene- och löphjulsregleringen har stor betydelse för kraftverkens frekvensregleringsarbete. Glappet gör att små regleråtgärder får större fasvridning och mindre amplitud än förväntat, vilket kan vara negativt för elnätets frekvenshållning. Mätningarna tydliggör också att reglerstyrkan från en anläggning är starkt beroende av driftpunkten, eftersom sambandet mellan uteffekt och pådrag inte är linjärt. Om systemoperatörerna ska få en bra uppfattning om hur mycket reglerstyrka som verkligen finns tillgänglig vid en viss tidpunkt så krävs det att kraftbolagen bygger sina beräkningar av reglerstyrkan på den aktuella punkten på turbinkurvan.

En jämförelse mellan den information om anläggningarnas dynamiska beteende som kan erhållas från olika typer av experiment (nätfrekvenssteg, nätfrekvenssinusvåg och börvärdesändring) görs också. Sinusformad nätfrekvenssignal med olika periodtider visar sig ge mest information om glappet och om systemets dynamik för övrigt, och kan därför rekommenderas.

Informationen om anläggningarnas dynamik används sedan för att optimera primärregleringens reglerparametrar. Mål för robusthet, störningskänslighet och prestanda sätts upp i frekvensdomän och reglerparametrarna optimeras i ett system där alla frekvensreglerande vattenkraftverk klumpas ihop till ett. Resultaten visar att undertryckningen av störningar med periodtider kring 40-90 sekunder kan förbättras så att den kvarvarande amplituden nästan halveras jämfört med dagens regulator (Vattenfalls Ep0-inställingar används som jämförelse). Den viktigaste åtgärden för att åstadkomma detta är att öka proportionaldelen i turbinregulatorn, det vill säga öka regulatorns omedelbara svar på frekvensavvikelser. Det optimala parametervalet beror också på systemets parametrar, vars värden i viss mån är osäkra. Om elnätets rotationströghet är låg är det mer lämpligt med en långsammare regulator, förutsatt att de uppställda kraven för känslighet och robusthet ska uppfyllas. För ett kraftverk med en längre vattentidskontant är det också lämpligt med en långsammare regulator, medan en snabbare regulator kan väljas för ett system med hög rotationströghet och för kraftverk med korta vattentidskonstanter.

References

[1] I. Pierre, F. Bauer, R. Blasko, N. Dahlbäck, M. Dumpelmann, K. Kainurinne, S. Luedge, P. Opdenacker, I. Pescador Chamorro, D. Romano, F. Schoonacker, and G. Weisrock, "Flexible generation: Backing up renewables," Eurelectric, Tech. Rep., 2011.

[2] B. Ummels, M. Gibescu, E. Pelgrum, W. Kling, and A. Brand, "Impacts of wind power on thermal generation unit commitment and dispatch," *IEEE Transactions on Energy Conversion*, vol. 22, no. 1, pp. 44 –51, march 2007.

[3] D. Heide, L. von Bremen, M. Greiner, C. Hoffmann, M. Speckmann, and S. Bofinger, "Seasonal optimal mix of wind and solar power in a future, highly renewable europe," *Renewable Energy*, vol. 35, no. 11, pp. 2483 – 2489, 2010.

[4] D. Heide, M. Greiner, L. von Bremen, and C. Hoffmann, "Reduced storage and balancing needs in a fully renewable european power system with excess wind and solar power generation," *Renewable Energy*, vol. 36, no. 9, pp. 2515 – 2523, 2011.

[5] M. G. Rasmussen, G. B. Andresen, and M. Greiner, "Storage and balancing synergies in a fully or highly renewable pan-european power system," *Energy Policy*, vol. 51, no. 0, pp. 642 – 651, 2012, renewable Energy in China.

[6] K. Hedegaard and P. Meibom, "Wind power impacts and electricity storage - a time scale perspective," *Renewable Energy*, vol. 37, no. 1, pp. 318 – 324, 2012.

[7] J. O. Tande and M. Korpås, "Impact of large scale wind power on system adequacy in a regional interconnections," in *Nordic wind power conference*, May 2006.

[8] Y. Makarov, P. Du, M. Kintner-Meyer, C. Jin, and H. Illian, "Sizing energy storage to accommodate high penetration of variable energy resources," *IEEE Transactions on Sustainable Energy*, vol. 3, no. 1, pp. 34 –40, jan. 2012.

[9] M. Black and G. Strbac, "Value of bulk energy storage for managing wind power fluctuations," *IEEE Transactions on Energy Conversion*, vol. 22, no. 1, pp. 197 –205, march 2007.

[10] E. D. Castronuovo and J. ao A. Peças Lopes, "Optimal operation and hydro storage sizing of a wind-hydro power plant," *International Journal of Electrical Power and Energy Systems*, vol. 26, no. 10, pp. 771 – 778, 2004.

[11] J. S. Anagnostopoulos and D. E. Papantonis, "Pumping station design for a pumped-storage wind-hydro power plant," *Energy Conversion and Management*, vol. 48, no. 11, pp. 3009 – 3017, 2007, 19th International Conference on Efficiency, Cost, Optimization, Simulation and Environmental Impact of Energy Systems.

[12] L. V. L. Abreu, M. E. Khodayar, M. Shahidehpour, and L. Wu, "Risk-constrained coordination of cascaded hydro units with variable wind power generation," *IEEE Transactions on Sustainable Energy*, vol. 3, no. 3, pp. 359 –368, july 2012.

[13] B. Hartmann and A. Dan, "Cooperation of a grid-connected wind farm and an energy storage unit ;demonstration of a simulation tool," *IEEE Transactions on Sustainable Energy*, vol. 3, no. 1, pp. 49 –56, jan. 2012.
[14] P. Pinson, G. Papaefthymiou, B. Klockl, and J. Verboomen, "Dynamic sizing of energy storage for hedging wind power forecast uncertainty," in *Power Energy Society General Meeting, 2009. PES '09. IEEE*, july 2009, pp. 1 –8.
[15] H. Holttinen, "Impact of hourly wind power variations on the system operation in the nordic countries," *Wind Energy*, vol. 8, no. 2, pp. 197–218, 2005.
[16] P. Sorensen, N. Cutululis, A. Vigueras-Rodriguez, L. Jensen, J. Hjerrild, M. Donovan, and H. Madsen, "Power fluctuations from large wind farms," *IEEE Transactions on Power Systems*, vol. 22, no. 3, pp. 958 –965, aug. 2007.
[17] I. Margaris, S. Papathanassiou, N. Hatziargyriou, A. Hansen, and P. Sorensen, "Frequency control in autonomous power systems with high wind power penetration," *IEEE Transactions on Sustainable Energy*, vol. 3, no. 2, pp. 189 –199, april 2012.
[18] F. Kreikebaum, R. Moghe, A. Prasai, and D. Divan, "Evaluating the application of energy storage and day-ahead solar forecasting to firm the output of a photovoltaic plant," in *Energy Conversion Congress and Exposition (ECCE), 2011 IEEE*, sept. 2011, pp. 3556 –3561.
[19] H. Shayeghi, H. Shayanfar, and A. Jalili, "Load frequency control strategies: A state-of-the-art survey for the researcher," *Energy Conversion and Management*, vol. 50, no. 2, pp. 344 – 353, 2009.
[20] S. K. Pandey, S. R. Mohanty, and N. Kishor, "A literature survey on load frequency control for conventional and distribution generation power systems," *Renewable and Sustainable Energy Reviews*, vol. 25, no. 0, pp. 318 – 334, 2013.
[21] H. E. Wichert and N. S. Dhaliwal, "Analysis of P.I.D. governors in multimachine system," *IEEE Transactions on Power Apparatus and Systems*, vol. PAS-97, no. 2, pp. 456–463, March 1978.
[22] S. Hagihara, H. Yokota, K. Goda, and K. Isobe, "Stability of a hydraulic turbine generating unit controlled by P.I.D. governor," *IEEE Transactions on Power Apparatus and Systems*, vol. PAS-98, no. 6, pp. 2294–2298, Nov 1979.
[23] G. Orelind, L. Wozniak, J. Medanic, and T. Whittemore, "Optimal PID gain schedule for hydrogenerators-design and application," *IEEE Power Engineering Review*, vol. 9, no. 9, pp. 31–31, Sept 1989.
[24] Y. Wang, R. Zhou, and C. Wen, "Robust load-frequency controller design for power systems," *IEE Proceedings Generation, Transmission and Distribution*, vol. 140, no. 1, pp. 11–16, Jan 1993.
[25] J. Jiang, "Design of an optimal robust governor for hydraulic turbine generating units," *IEEE Transactions on Energy Conversion*, vol. 10, no. 1, pp. 188–194, Mar 1995.
[26] K. Lim, Y. Wang, and R. Zhou, "Robust decentralised load-frequency control of multi-area power systems," *IEE Proceedings Generation, Transmission and Distribution*, vol. 143, no. 5, pp. 377–386, Sep 1996.
[27] R. K. Sahu, S. Panda, and U. K. Rout, "DE optimized parallel 2-DOF PID controller for load frequency control of power system with governor dead-band nonlinearity," *International Journal of Electrical Power & Energy Systems*, vol. 49, no. 0, pp. 19 – 33, 2013.

[28] K. Natarajan, "Robust PID controller design for hydroturbines," *IEEE Transactions on Energy Conversion*, vol. 20, no. 3, pp. 661–667, Sept 2005.
[29] A. Stanković, G. Tadmor, and T. Sakharuk, "On robust control analysis and design for load frequency regulation," *IEEE Transactions on Power Systems*, vol. 13, no. 2, pp. 449–455, May 1998.
[30] W. Tan, "Tuning of PID load frequency controller for power systems," *Energy Conversion and Management*, vol. 50, no. 6, pp. 1465 – 1472, 2009.
[31] A. Khodabakhshian and R. Hooshmand, "A new PID controller design for automatic generation control of hydro power systems," *International Journal of Electrical Power & Energy Systems*, vol. 32, no. 5, pp. 375 – 382, 2010.
[32] K. S. Parmar, S. Majhi, and D. Kothari, "Load frequency control of a realistic power system with multi-source power generation," *International Journal of Electrical Power & Energy Systems*, vol. 42, no. 1, pp. 426 – 433, 2012.
[33] P. Hušek, "PID controller design for hydraulic turbine based on sensitivity margin specifications," *International Journal of Electrical Power & Energy Systems*, vol. 55, no. 0, pp. 460 – 466, 2014.
[34] M. Toulabi, M. Shiroei, and A. Ranjbar, "Robust analysis and design of power system load frequency control using the kharitonov's theorem," *International Journal of Electrical Power & Energy Systems*, vol. 55, no. 0, pp. 51 – 58, 2014.
[35] W. Tan and H. Zhou, "Robust analysis of decentralized load frequency control for multi-area power systems," *International Journal of Electrical Power & Energy Systems*, vol. 43, no. 1, pp. 996 – 1005, 2012.
[36] H. Fang, L. Chen, N. Dlakavu, and Z. Shen, "Basic modeling and simulation tool for analysis of hydraulic transients in hydroelectric power plants," *IEEE Transactions on Energy Conversion,*, vol. 23, no. 3, pp. 834–841, Sept 2008.
[37] G. Robert and F. Michaud, "Hydro power plant modeling for generation control applications," in *American Control Conference (ACC), 2012*, June 2012, pp. 2289–2294.
[38] P. Kundur, N. J. Balu, and M. G. Lauby, *Power system stability and control*. New York: McGraw-Hill, 1994.
[39] C. Vournas and G. Papaioannou, "Modelling and stability of a hydro plant with two surge tanks," *IEEE Transactions on Energy Conversion,*, vol. 10, no. 2, pp. 368–375, Jun 1995.
[40] G. Munoz-Hernandez and D. Jones, "Mimo generalized predictive control for a hydroelectric power station," *IEEE Transactions on Energy Conversion,*, vol. 21, no. 4, pp. 921–929, Dec 2006.
[41] D. Arnautović and R. Milijanović, "An approach to the analysis of large perturbations in hydro-electric plants with kaplan turbines," *Electric Power Systems Research*, vol. 9, no. 2, pp. 115 – 121, 1985.
[42] D. Kosterev, "Hydro turbine-governor model validation in pacific northwest," *IEEE Transactions on Power Systems,*, vol. 19, no. 2, pp. 1144–1149, May 2004.
[43] L. Hannett, J. Feltes, and B. Fardanesh, "Field tests to validate hydro turbine-governor model structure and parameters," *IEEE Transactions on Power Systems,*, vol. 9, no. 4, pp. 1744–1751, Nov 1994.
[44] S. Patterson, "Importance of hydro generation response resulting from the new thermal modeling -and required hydro modeling improvements," in *IEEE Power*

Engineering Society General Meeting, 2004., June 2004, pp. 1779–1783 Vol.2.
[45] E. Agneholm, "Measures to mitigate the frequency oscillations with a period of 60-90 seconds in the nordic synchronous system," Gothia Power, Tech. Rep., 2013.
[46] D. Jones, S. Mansoor, F. Aris, G. Jones, D. Bradley, and D. King, "A standard method for specifying the response of hydroelectric plant in frequency-control mode," *Electric Power Systems Research*, vol. 68, no. 1, pp. 19 – 32, 2004. [Online]. Available: http://www.sciencedirect.com/science/article/pii/S0378779603001524
[47] G. Bryce, P. Agnew, T. R. Foord, D. Winning, and A. Marshal, "On-site investigation of electrohydraulic governors for water turbines," *Proceedings of the Institution of Electrical Engineers,*, vol. 124, no. 2, pp. 147–153, February 1977.
[48] A. Klopfenstein, "Response of steam and hydroelectric generating plants to generation control tests," *Power Apparatus and Systems, Part III. Transactions of the American Institute of Electrical Engineers*, vol. 78, no. 4, pp. 1371–1376, Dec 1959.
[49] R. Oldenburger and J. Donelson, "Dynamic response of a hydroelectric plant," *Power Apparatus and Systems, Part III. Transactions of the American Institute of Electrical Engineers*, vol. 81, no. 3, pp. 403–418, April 1962.
[50] "Guidelines for generator stability model validation testing," in *IEEE Power Engineering Society General Meeting, 2006*., 2006, pp. 6 pp.–.
[51] L. Ljung and T. Glad, *Modellbygge och simulering*. Lund: Studentlitteratur, 2004.
[52] T. Glad and L. Ljung, *Control theory : multivariable and nonlinear methods*. London: Taylor & Francis, 2000.
[53] L. Söder, "På väg mot en elförsörjningbaserad på enbart förnybar el i sverige : En studie om behov av reglerkraft och överföringskapacitet. version 4.0," Tech. Rep., 2014.
[54] I. Argyrakis, V. Vladislav Babkin, M. Chudy, G. Crosnier, N. Dahlbäck, R. Gianatti, P. Gomez Martin, E. G. Gudnason, K. Hellsten, G. Kreiss, I. Nikolov, P. Oesch, B. o'Mahony, R. Pala, L. Reinig, D. Kreikenbaum, D. Polak, N. Romer, Z. Saturka, V. Stanojevic, A. Stettler, C. Marin, J. C. T. Freitas, J. Lobacz, G. Weisrock, J. Jenko, K. SEELOS, and M. Timm, "Hydro in europe: Powering renewables," Eurelectric, Tech. Rep., 2011.
[55] NordPool. (2012, Augusti) Reservoir content for electrical exchange area. Internet. [Online]. Available: http://www.nordpoolspot.com
[56] "Matlab system identification toolbox," http://www.mathworks.se/products/sysid/, The Mathworks Inc., May 2014.
[57] K. J. Åström and T. Hägglund, *Advanced PID control*. Research Triangle Park, NC, USA: ISA-The Instrumentation, Systems, and Automation Society, 2006.
[58] "Matlab robust control toolbox," http://www.mathworks.se/help/robust/index.html, Mathworks, Inc., August 2014.
[59] T. Lysfjord, T. Keränen, L. Messing, T. Østrup, and B. Ingermars, "Förbättrad dämpning av effektpendlingar i nordelnätet genom optimering av inställbara reglerparametrar för dämptillsatser," Statens Vattenfallsverk, Tech. Rep., 1982.

[60] R. A. Maher, I. A. Mohammed, and I. K. Ibraheem, "Polynomial based H_∞ robust governor for load frequency control in steam turbine power systems," *International Journal of Electrical Power & Energy Systems*, vol. 57, no. 0, pp. 311 – 317, 2014.

Kph, Trycksaksbolaget AB, Uppsala 2014